© 2019. Published by The Company of Biologists Ltd | Development (2019) 146, dev163618. doi:10.1242/dev.163618

STEM CELLS AND REGENERATION

RESEARCH ARTICLE

Cell-autonomous and redundant roles of Hey1 and HeyL in muscle stem cells: HeyL requires Hes1 to bind diverse DNA sites

Yu-taro Noguchi[1,*], Miki Nakamura[1,*], Nobumasa Hino[2], Jumpei Nogami[3], Sayaka Tsuji[2], Takahiko Sato[4], Lidan Zhang[1], Kazutake Tsujikawa[1], Toru Tanaka[2], Kohei Izawa[2], Yoshiaki Okada[2], Takefumi Doi[2], Hiroki Kokubo[5], Akihito Harada[3], Akiyoshi Uezumi[6], Manfred Gessler[7], Yasuyuki Ohkawa[3] and So-ichiro Fukada[1,‡]

ABSTRACT

The undifferentiated state of muscle stem (satellite) cells (MuSCs) is maintained by the canonical Notch pathway. Although three bHLH transcriptional factors, Hey1, HeyL and Hes1, are considered to be potential effectors of the Notch pathway exerting anti-myogenic effects, neither HeyL nor Hes1 inhibits myogenic differentiation of myogenic cell lines. Furthermore, whether these factors work redundantly or cooperatively is unknown. Here, we showed cell-autonomous functions of Hey1 and HeyL in MuSCs using conditional and genetic null mice. Analysis of cultured MuSCs revealed anti-myogenic activity of both HeyL and Hes1. We found that HeyL forms heterodimeric complexes with Hes1 in living cells. Moreover, our ChIP-seq experiments demonstrated that, compared with HeyL alone, the HeyL-Hes1 heterodimer binds with high affinity to specific sites in the chromatin, including the binding sites of Hey1. Finally, analyses of myogenin promoter activity showed that HeyL and Hes1 act synergistically to suppress myogenic differentiation. Collectively, these results suggest that HeyL and Hey1 function redundantly in MuSCs, and that HeyL requires Hes1 for effective DNA binding and biological activity.

KEY WORDS: Notch, Muscle stem cells, Skeletal muscle, Mouse

INTRODUCTION

A muscle satellite cell (MuSC) is a physiologically adult stem cell that has the ability to self-renew and produce abundant daughter cells called myoblasts (Collins et al., 2005; Lepper et al., 2011; Sacco et al., 2008; Sambasivan et al., 2011). In a steady state, MuSCs remain quiescent and undifferentiated. Loss of the MuSC pool results in myogenic regeneration defects; therefore, the maintenance of MuSCs is crucial for skeletal muscle homeostasis (Lepper et al., 2011; Sambasivan et al., 2011). Recent studies have revealed some of the molecules regulating the quiescent and undifferentiated state of adult MuSCs (Cheung and Rando, 2013; Fukada et al., 2013; Yamaguchi et al., 2015). Among them, the canonical Notch signaling has emerged as a major molecular mechanism underlying the maintenance of adult MuSCs.

The Notch signaling pathway is an evolutionarily conserved intercellular signaling system and is required for cell fate decisions and patterning events (Lai, 2004). The Notch receptor family consists of four members (Notch1-4). When a Notch receptor is activated by binding to a ligand (Delta-like and Jagged), the cleaved Notch receptor (the intracellular domain of the Notch receptor) translocates to the nucleus where it activates transcription of target genes through interaction with Rbp-J (also known as Cbf1) (Lai, 2004). This Rbp-J-mediated pathway represents the canonical Notch pathway. A pioneering study of Notch-mediated cell fate decision in mammalian cells was performed using the myogenic cell line C2C12 (Lindsell et al., 1995). Subsequent studies showed that canonical Notch signaling exhibits anti-myogenic functions in a myogenic cell line (Kato et al., 1997; Kuroda et al., 1999). However, the effector molecules exerting anti-myogenic function is still controversial (Buas et al., 2009).

As mentioned, the canonical Notch pathway is essential for maintaining MuSCs in a quiescent and undifferentiated state; in the absence of Rbp-J, MuSC numbers decline quickly, and the myogenic differentiation factors MyoD and myogenin are upregulated (Bjornson et al., 2012; Mourikis et al., 2012). Double conditional mutagenesis of *Notch1* and *Notch2* results in similar phenotypes to observations in *Rbp-J*-depleted MuSCs, indicating that the canonical Notch1/2–Rbp-J axis is a key pathway for adult MuSCs maintenance (Fujimaki et al., 2018). However, similar to the myogenic cell line, the downstream molecules for maintaining adult MuSCs remain to be elucidated.

The best-known primary targets of canonical Notch signaling are the Hes (Hairy and enhancer of split) and Hey (Hes-related, also known as Hesr/Herp/Hrt/Gridlock/Chf) families of the bHLH transcriptional repressor genes, raising the question of whether these factors mediate Notch signals to suppress myogenic differentiation. However, previous analyses using a myogenic cell line, C2C12 cells, indicated that HeyL or Hes1 did not suppress the differentiation (Buas et al., 2009; Shawber et al., 1996). Furthermore, HeyL did not bind to the cis-element of Hey1 (Iso et al., 2003; Nakagawa et al., 2000), raising the question whether Hey1 and HeyL work redundantly. We reported previously that in *Hey1* and *HeyL* double knockout (dKO) mice, but not in *Hey1* or *HeyL* single KO mice, the generation of quiescent MuSCs was

[1]Laboratory of Molecular and Cellular Physiology, Graduate School of Pharmaceutical Sciences, Osaka University, 1-6 Yamadaoka, Suita, Osaka 565-0871, Japan. [2]Laboratory of Molecular Medicine, Graduate School of Pharmaceutical Sciences, Osaka University, 1-6 Yamadaoka, Suita, Osaka 565-0871, Japan. [3]Division of Transcriptomics, Medical Institute of Bioregulation, Kyushu University, Fukuoka 812-8582, Japan. [4]Department of Ophthalmology, Kyoto Prefectural University of Medicine, Kyoto 602-8566, Japan. [5]Department of Cardiovascular Physiology and Medicine, Graduate School of Biomedical and Health Sciences, Hiroshima University, 1-2-3 Kasumi, Minamiku, Hiroshima 734-8551, Japan. [6]Department of Geriatric Medicine, Tokyo Metropolitan Institute of Gerontology, Itabashi-ku, Tokyo 173-0015, Japan. [7]Developmental Biochemistry, Theodor-Boveri-Institute/Biocenter, and Comprehensive Cancer Center Mainfranken, University of Wuerzburg, 97074 Wuerzburg, Germany.
*These authors contributed equally to this work

‡Author for correspondence (fukada@phs.osaka-u.ac.jp)

M.N., 0000-0002-1977-0190; T.S., 0000-0003-3836-7978; L.Z., 0000-0001-5230-9016; A.U., 0000-0003-4294-0116; M.G., 0000-0002-7915-6045; Y.O., 0000-0001-6440-9954; S.-i.F., 0000-0003-4051-5108

Received 6 February 2018; Accepted 31 January 2019

Development (2019) 146, dev163618. doi:10.1242/dev.163618

impaired as a consequence of an increase in MyoD and myogenin expression (Fukada et al., 2011). This resembles the phenotypes of *Rbp-J* conditional KO (cKO) and *Notch1/2* double cKO mice (Bjornson et al., 2012; Fujimaki et al., 2018; Mourikis et al., 2012). In this study, genetically *Hey1*/*HeyL*-null mice were analyzed. *HeyL* is specifically expressed in MuSCs, but *Hey1* is also expressed in endothelial cells (Fukada et al., 2011) of the skeletal muscle, giving rise to the possibility of non-cell-autonomous roles of Hey1 in the muscle. We therefore used conditional mutagenesis to demonstrate that Hey1/HeyL are required in a cell-autonomous manner for maintenance of MuSCs, and that in the absence of Hey1/HeyL the cells upregulate MyoD and myogenin. Moreover, we investigate the mechanisms of Hey1/HeyL redundant functions and demonstrate that these factors form heterodimers with Hes1, and that, in particular, HeyL requires Hes1 in order to bind with a higher affinity to chromatin and repress myogenesis more efficiently. Our results explain the controversial findings that Notch signaling induces HeyL and Hes1; however, neither HeyL nor Hes1 can suppress differentiation alone, thus indicating that HeyL cooperates with Hes1.

RESULTS

Hey1/HeyL are essential for maintaining the muscle satellite cell pool in adult skeletal muscle

In order to ensure the cell-autonomous and redundant roles of Hey1 and HeyL in MuSCs, it was necessary to use MuSC-specific conditional KO mice. In skeletal muscle, *HeyL* mRNA is exclusively expressed in MuSCs, similar to *Myf5* and *Pax7*. But *Hey1* mRNA is also detected in CD31 (Pecam1)-positive endothelial cells (Fig. S1A) (Fukada et al., 2011). Additionally, single *HeyL* KO mice do not show significant phenotypes, even in skeletal muscle and heart (Fischer et al., 2007; Fukada et al., 2011). Therefore, we conditionally depleted the *Hey1* gene in MuSCs using $Pax7^{CreERT2/+}$ mice (Lepper et al., 2009).

Hey1/HeyL double-knockout (hereafter referred as dKO) mice used in previous studies showed decreased body weight and size. MuSC number was already reduced by 7 days after birth (Fukada et al., 2011). In contrast to dKO mice, MuSC-specific conditional *Hey1/HeyL* dKO mice treated with tamoxifen (Tm) (hereafter referred as co-dKO; $Pax7^{CreERT2/+}$::$Hey1^{flox/-}$ or $^{flox/flox}$::$HeyL^{-/-}$ mice with Tm) did not exhibit apparent impairments. The body and muscle weight of co-dKO mice were comparable to those of littermate controls (Fig. 1A). However, MuSC numbers were significantly reduced in co-dKO mice compared with control mice 3 weeks after Tm injection (Fig. 1B). The cell size of co-dKO MuSCs was larger than that of control MuSCs (Fig. 1B,C).

Next, we examined the time dependency of the effect of Tm injection on MuSCs. Unexpectedly, when we used mice older than 8 weeks, conditional *Hey1/HeyL* double mutant mice untreated with Tm (hereafter referred as co-dMt; $Pax7^{CreERT2/+}$::$Hey1^{flox/-}$ or $^{flox/flox}$::$HeyL^{-/-}$ mice without Tm) mice showed a reduction in the number of MuSCs and in *Hey1* transcripts (Fig. 1D, Fig. S1A). However, 4-week-old co-dMt mice showed normal MuSCs numbers and *Hey1* transcript levels (Fig. 1D, Fig. S1B), indicating that the MuSC pool in co-dMt mice was not affected during postnatal development in contrast to the phenotype of dKO mice, but the MuSC pool is not sustained in the absence of both Hey1 and HeyL.

The loss of MuSCs results in impaired muscle regeneration. As shown in Fig. 1E-H, both reduced weight of regenerated muscle and increased area of fibrosis were observed in co-dKO mice. Because our previous analyses of dKO MuSCs indicated that the absence of both Hey1 and HeyL had no impact on MuSC proliferation and myotube formation (Fukada et al., 2011), the impaired regeneration in co-dKO could result from the loss of the MuSC pool in co-dKO mice. Taken together, an unexpected reduction of *Hey1* in the Tm-untreated mice occurred after co-dMt mice were 4 weeks old. Because the MuSC pool is established about 3 weeks after birth (White et al., 2010), our studies demonstrate that Hey1 and HeyL are essential for maintaining the MuSC pool via cell-autonomous effects, in addition to their roles in generating adult MuSCs.

Impaired quiescent and undifferentiated state in conditional *Hey1*/*HeyL* KO MuSCs

To examine the effect of the absence of Hey1 and HeyL on the undifferentiated state of MuSCs, the expression of the myogenic differentiation markers MyoD and myogenin was investigated. As shown in Fig. 2A,B, an increased number of $MyoD^+$ or $myogenin^+$ cells was detected in skeletal muscle sections of co-dKO mice. Consistent with Fig. 1D, a decrease in the number of MuSCs on isolated single myofibers was observed in >4-week-old co-dMt mice. In addition, analyses of isolated single myofibers also indicated increased $MyoD^+$ or $myogenin^+$ cells in co-dMt mice (9 weeks old; Fig. 2C,D).

Next, we examined the mRNA expression of *Myod* and myogenin together with two other myogenic genes, *Myf5* and *Pax7*. Significantly increased expression of the myogenin gene was observed in both dKO and co-dKO/co-dMt MuSCs, but not in control and single KO mice (Fig. 2E,F), suggesting redundant roles of Hey1 and HeyL in MuSCs. mRNA expression levels of *Myf5* was decreased or tended to decrease in dKO and co-dKO/co-dMt MuSC (Fig. 2E,F). Hey1 and HeyL are considered to be transcriptional repressors (Heisig et al., 2012); therefore, these results suggest that the accelerated myogenic differentiation secondarily affected *Myf5* expression in co-dKO/co-dMt mice (Machado et al., 2017). Decreased expression of *Pax7* was observed in co-dMt MuSCs, but not in dKO and co-dKO MuSCs. One possibility is that one allele of *Pax7* was not transcribed in co-dMt compared with the control mice ($Hey1^{flox/flox}$ or $^{flox/+}$::$HeyL^{-/-}$ mice). Therefore, the genetic construct might have resulted in the decreased *Pax7* expression in co-dMt. The *Myod* mRNA expression level was not changed in either dKO or co-dKO/co-dMt compared with control or single KO mice.

Anti-myogenic effects of Hey1, HeyL and Hes1 in primary myoblasts

Our data demonstrate that Hey1 and HeyL function redundantly to maintain the undifferentiated state of MuSCs *in vivo*. However, HeyL did not exhibit remarkable anti-myogenic effects in a myogenic cell line (C2C12), as observed with Hey1 (Fig. S2) (Buas et al., 2009). Hes1, another important target of Notch signaling, also does not have an anti-myogenic effect in C2C12 (Fig. S2) (Shawber et al., 1996). In order to examine the impact of Hey1, HeyL and Hes1 on primary myoblasts, each gene was retrovirally expressed in primary myoblasts, and MyoD expression was quantified. As shown in Fig. 3A,B, both the percentage of MyoD-positive cells and *Myod* mRNA expression were significantly reduced by Hey1 expression, indicating that Hey1 had a significant anti-myogenic effect on primary myoblasts, as observed in C2C12. On the other hand, HeyL did not alter the percentage of MyoD-positive cells, but increased the number of MyoD-low cells and suppressed *Myod* mRNA expression (Fig. 3A,B). Furthermore, HeyL slightly, but significantly, reduced myotube formation (Fig. 3C), indicating that HeyL has anti-myogenic effects on

Development (2019) 146, dev163618. doi:10.1242/dev.163618

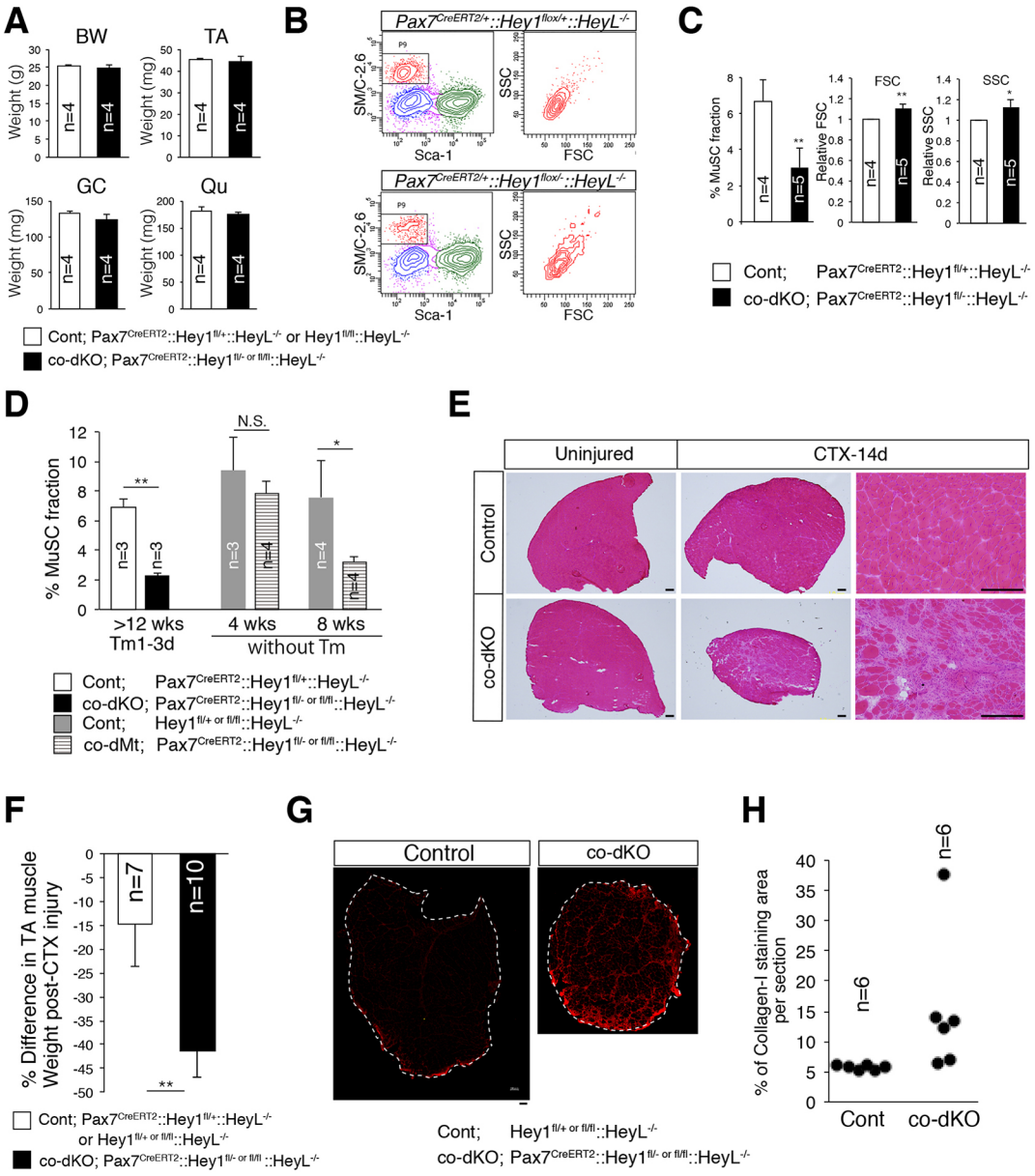

Fig. 1. Muscle stem cell numbers and regenerative ability are reduced in conditional *Hey1*/*HeyL* double knockout mice. (A) Body weight (BW) and tibialis anterior (TA), gastrocnemius (GC) and quadriceps (Qu) muscle weights of control (white bar: *Pax7*$^{CreERT2/+}$*::Hey1*$^{flox/+}$*::HeyL*$^{-/-}$ or *Hey1*$^{flox/flox}$*::HeyL*$^{-/-}$) or co-dKO (black bar: *Pax7*$^{CreERT2/+}$*::Hey1*$^{flox/-}$ or *flox/flox*::*HeyL*$^{-/-}$) male mice at 10 weeks old, 2 weeks after Tm injection. The *y*-axis shows the mean with s.d. (B) FACS profiles of mononuclear cells derived from control (*Pax7*$^{CreERT2/+}$*::Hey1*$^{flox/+}$*::HeyL*$^{-/-}$) or co-dKO (*Pax7*$^{CreERT2/+}$*::Hey1*$^{flox/-}$*::HeyL*$^{-/-}$) muscles. The left profiles were gated for CD31$^-$ CD45$^-$ fractions. The right profiles show the cell size (FSC) and cell granularity (SSC) of MuSC fractions (SM/C-2.6$^+$CD31$^-$CD45$^-$Sca1$^-$). (C) The mean percentage, the relative forward scatter (FSC), or the relative side scatter (SSC) of MuSC derived from control (*Pax7*$^{CreERT2/+}$*::Hey1*$^{flox/+}$*::HeyL*$^{-/-}$) or co-dKO (*Pax7*$^{CreERT2/+}$*::Hey1*$^{flox/-}$*::HeyL*$^{-/-}$) muscles 7-19 days after Tm injection. (D) Quantitative analyses of MuSC number by flow cytometer. The *y*-axis shows the percentage of SM/C-2.6$^+$CD31$^-$CD45$^-$Sca1$^-$ cells in control (white bar: *Pax7*$^{CreERT2/+}$*::Hey1*$^{flox/+}$*::HeyL*$^{-/-}$, 1-3 days after Tm; gray bar: *Hey1*$^{flox/flox}$ or *flox/+*::*HeyL*$^{-/-}$, without injection Tm), co-dKO mice (black bar: *Pax7*$^{CreERT2/+}$*::Hey1*$^{flox/-}$ or *flox/flox*::*HeyL*$^{-/-}$, 1-3 days after Tm), or co-dMt (striped bar: *Pax7*$^{CreERT2/+}$*::Hey1*$^{flox/-}$ or *flox/flox*::*HeyL*$^{-/-}$ without Tm) at the indicated age or date. The *x*-axis shows the mean with s.d. (E) Histological analyses (H&E staining) of control (*Hey1*$^{flox/+}$*:HeyL*$^{-/-}$) and co-dKO (*Pax7*$^{CreERT2/+}$*::Hey1*$^{flox/-}$*::HeyL*$^{-/-}$) muscles 2 weeks after cardiotoxin (CTX) injection. Scale bar: 200 µm. (F) The change in TA muscle weight 2 weeks after CTX injection in control (white bar: *Pax7*$^{CreERT2/+}$*::Hey1*$^{flox/+}$*::HeyL*$^{-/-}$ or *Hey1*$^{flox/flox}$ or *flox/+*::*HeyL*$^{-/-}$, 5 weeks after Tm injection) or co-dKO (black bar: *Pax7*$^{CreERT2/+}$*::Hey1*$^{flox/-}$ or *flox/flox*::*HeyL*$^{-/-}$, 5 weeks after Tm injection) mice. Tm injection was carried out at 10-16 weeks of age. (G) Immunohistochemical staining for collagen type I (red) in control (*Hey1*$^{flox/+}$*::HeyL*$^{-/-}$, 5 weeks after Tm injection) or co-dKO (*Pax7*$^{CreERT2/+}$*::Hey1*$^{flox/flox}$*::HeyL*$^{-/-}$, 5 weeks after Tm injection) muscle 2 weeks after CTX injection. Dashed line outlines the section of TA muscle. Scale bar: 100 µm. (H) Quantitative analyses of the collagen I-positive area per section in control (*Hey1*$^{flox/flox}$ or *flox/+*::*HeyL*$^{-/-}$; 5 weeks after Tm) and co-dKO mice (*Pax7*$^{CreERT2/+}$*::Hey1*$^{flox/-}$ or *flox/flox*::*HeyL*$^{-/-}$; 5 weeks after Tm injection) 2 weeks after CTX injection. Tm injection was carried out at 10-16 weeks of age. The numbers of mice analyzed per group are shown on the graphs. N.S., not significant; *P<0.05; **P<0.01.

primary myoblasts. Hes1 remarkably suppressed the MyoD level in primary myoblasts (Fig. 3D). Taken together, although HeyL and Hes1 were considered to have no anti-myogenic effect based on the study of C2C12 cells, these results indicate that both HeyL and Hes1 exerted an anti-myogenic effect in a more physiological type of cell, primary myoblasts, as observed by another group (Wen et al., 2012).

Development (2019) 146, dev163618. doi:10.1242/dev.163618

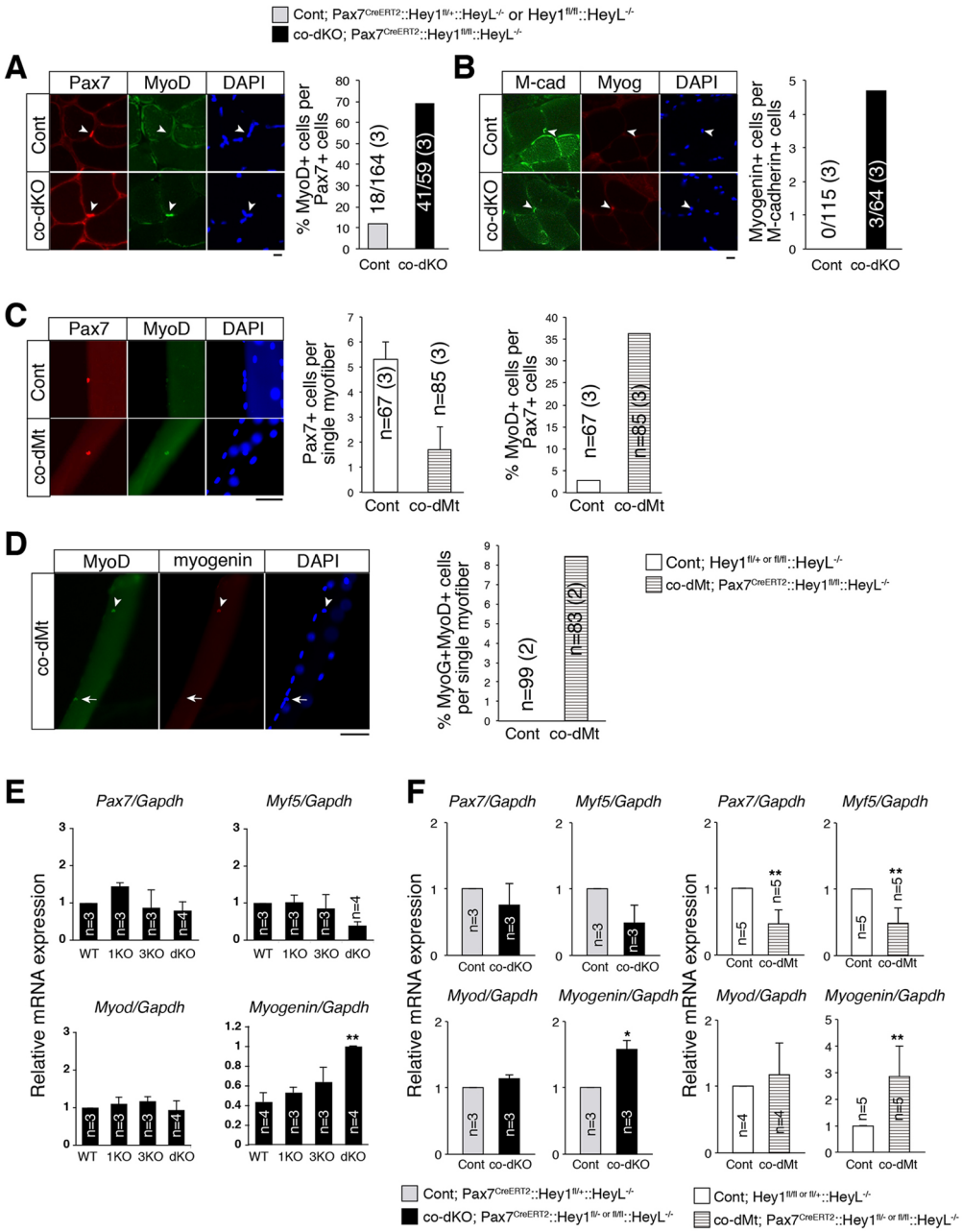

Fig. 2. The **undifferentiated state is impaired in *Hey1*/*HeyL*-conditional KO mice.** (A) Uninjured TA muscles of control and co-dKO mice at 10 weeks old were stained with anti-Pax7 (red) and anti-MyoD (green) antibodies. Arrowheads show muscle stem cells. The graph indicates the frequency of MyoD$^+$ cells as a percentage of total Pax7$^+$ cells in control (gray bar: *Pax7*$^{CreERT2/+}$*::Hey1*$^{flox/+}$*::HeyL*$^{-/-}$ or *Hey1*$^{flox/flox}$*::HeyL*$^{-/-}$, 2 weeks after Tm injection) and co-dKO mice (black bar: *Pax7*$^{CreERT2/+}$*::Hey1*$^{flox/flox}$*::HeyL*$^{-/-}$, 2 weeks after Tm injection). The number of marker-positive MuSCs among total counted MuSCs is indicated for each bar. The number in parentheses shows the number of mice used for analyses. (B) Uninjured TA muscles of 10-week-old control and co-dKO mice were stained with anti-M-cadherin (M-cad; green) and myogenin (Myog; red) antibodies. Arrowheads show muscle stem cells. The graph indicates the frequency of myogenin$^+$ cells as a percentage of total M-cadherin$^+$ cells in control (gray bar: *Pax7*$^{CreERT2/+}$*::Hey1*$^{flox/+}$*::HeyL*$^{-/-}$ or *Hey1*$^{flox/flox}$*::HeyL*$^{-/-}$, 2 weeks after Tm injection) and co-dKO (black bar: *Pax7*$^{CreERT2/+}$*::Hey1*$^{flox/flox}$*::HeyL*$^{-/-}$, 2 weeks after Tm injection) mice. The number of marker-positive MuSCs among total counted MuSCs is indicated for each bar. The number in parentheses shows the number of mice used for analyses. (C) Freshly isolated single myofibers were stained with anti-Pax7 (red) and anti-MyoD (green) antibodies. The graphs indicate the number of Pax7$^+$ cells per single myofiber or the percentage of MyoD$^+$ cells out of total Pax7$^+$ cells in control (white bar: *Hey1*$^{flox/flox}$ or $^{flox/+}$*::HeyL*$^{-/-}$) and co-dMt (striped bar: *Pax7*$^{CreERT2/+}$*::Hey1*$^{flox/flox}$*::HeyL*$^{-/-}$) mice. The number of myofibers counted is indicated for each bar. The number in parentheses shows the number of mice used for analyses. Nine-week-old mice were used. (D) Freshly isolated single myofibers were stained with anti-MyoD (green) and anti-myogenin (red) antibodies. Arrowheads and arrows show MyoD$^+$/myogenin$^+$ and MyoD$^+$/myogenin$^-$ cells, respectively. The graph indicates the percentage of MyoD$^+$myogenin$^+$ cells per single myofiber in control (white bar: *Hey1*$^{flox/flox}$*::HeyL*$^{-/-}$) and co-dMt (striped bar: *Pax7*$^{CreERT2/+}$*::Hey1*$^{flox/flox}$*::HeyL*$^{-/-}$) mice. The number of myofibers counted is indicated for each bar. The number in parentheses shows the number of mice used for analyses. Nine-week-old mice were used. (E) Relative mRNA expression of myogenic genes in freshly isolated MuSCs derived from wild-type (WT), Hey1-KO (1KO), HeyL-KO (3KO) or Hey1/HeyL-dKO (dKO) mice. Ten- to 12-week-old mice were used. (F) Relative mRNA expression of myogenic genes in freshly isolated MuSCs derived from control (gray bars: *Pax7*$^{CreERT2/+}$*::Hey1*$^{flox/+}$*::HeyL*$^{-/-}$ 2 weeks after Tm), co-dKO (black bars: *Pax7*$^{CreERT2/+}$*::Hey1*$^{flox/flox}$ or $^{flox/-}$*::HeyL*$^{-/-}$ 2 weeks after Tm), control (white bars: *Hey1*$^{flox/flox}$ or $^{flox/+}$*::HeyL*$^{-/-}$ without Tm), or co-dMt (striped bars: *Pax7*$^{CreERT2/+}$*::Hey1*$^{flox/flox}$ or $^{flox/-}$*::HeyL*$^{-/-}$ without Tm) mice. Eight- to 14-week-old mice were analyzed in this study. *P<0.05; **P<0.01. Scale bars: 10 µm (A,B); 50 µm (C,D).

Development (2019) 146, dev163618. doi:10.1242/dev.163618

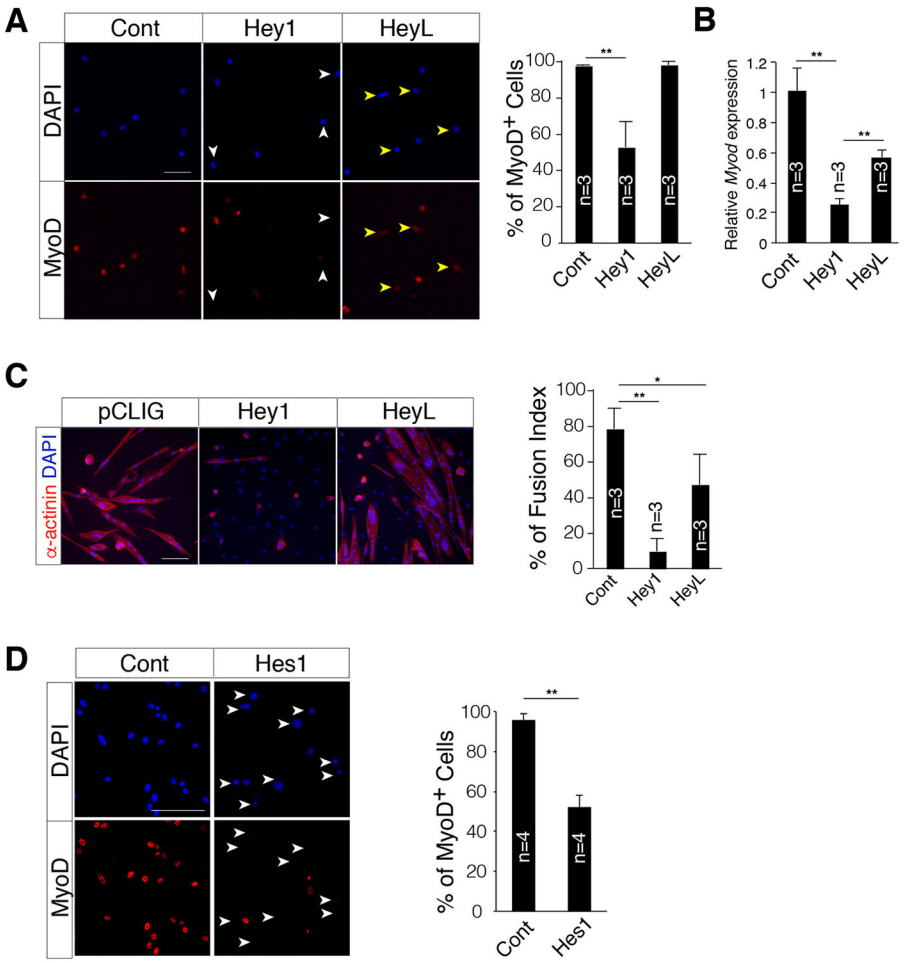

Fig. 3. HeyL and Hes1 show an anti-myogenic effect in primary myoblasts. (A) Proliferating MuSCs were infected with one of the following retrovirus constructs: parental vector expressing GFP (control; Cont); Hey1- and GFP-expressing vector (Hey1); HeyL- and GFP-expressing vector (HeyL). Sorted and cultured GFP$^+$ cells were stained for MyoD. White and yellow arrowheads indicate MyoD$^-$ and MyoD^{low} cells, respectively. The graph indicates the percentage of MyoD$^+$ cells out of total Cont, Hey1-, or HeyL-expressing cells obtained from three independent experiments. (B) Relative mRNA expression of *Myod* in Cont, Hey1-, or HeyL-expressing cells obtained from three independent experiments. (C) Immunostaining for alpha-sarcomeric actinin (red). The graph shows the fusion index of Cont, Hey1- or HeyL-expressing cells. (D) Proliferating MuSCs were infected with each retrovirus construct: parental vector expressing GFP (Cont); Hes1- and GFP-expressing vector (Hes1). Sorted and cultured GFP$^+$ cells were stained for MyoD. Arrowheads indicate MyoD$^-$ cells. The graph indicates the percentage of MyoD$^+$ cells out of total Cont or Hes1-expressing cells obtained from four independent experiments. *P<0.05; **P<0.01. Scale bars: 100 µm.

HeyL and Hes1 form heterodimers in living cells

The different effects of HeyL and Hes1 on primary myoblasts and the C2C12 cell line implied three possibilities: (1) the absence of a co-repressor for Hes1 or HeyL in C2C12 cells, (2) the absence of each heterodimer partner in C2C12 cells, or (3) both. Thus, we examined the necessity of Hes1 for HeyL because it is possible that Hes1 and HeyL work as a heterodimer (Jalali et al., 2011). First, we assayed the existence of HeyL-Hes1 heterodimers in living cells using a site-specific photo-crosslink technique (Hino et al., 2005; Kita et al., 2016) (Fig. 4A). For successful photo-crosslinking between interacting proteins, a photo-crosslinkable amino acid, Nε-(meta-trifluoromethyl-diazirinyl-benzyloxycarbonyl)-l-lysine (mTmdZLys), should be incorporated near the binding interface of the proteins. We decided to introduce mTmdZLys into the Orange and bHLH domains of HeyL at the positions indicated in Fig. 4B,C because Hey and Hes1 form homodimers via these domains (Iso et al., 2001), and formation of heterodimers of the proteins via the same domains was expected. Each mTmdZLys-containing and C-terminal FLAG-tagged HeyL mutant was expressed in 293 c18 cells, together with C-terminal Myc-tagged Hes1 protein. After exposure of the cells to UV light, HeyL complexes were purified from extracts of the cells with an anti-FLAG antibody, and then analyzed by western blotting with an anti-Myc antibody. As shown in Fig. 4D, a product with a molecular mass of ∼70 kDa, which almost corresponds to the sum of the masses of HeyL (35 kDa) and Hes1 (30 kDa), was detected depending on the exposure to UV light. This result indicates photo-crosslinking of HeyL with Hes1, i.e. heterodimer formation of the proteins in living cells. A similar result was obtained for Hey1, indicating heterodimerization with Hes1 (Fig. 4B,C,E). Hey1 and HeyL also formed a heterodimer complex (Fig. S3A). On the other hand, neither Hey1 nor HeyL formed heterodimers with MyoD (Fig. 4F,G), and Hes1 formed a heterodimer with MyoD much less efficiently than with HeyL (Fig. 4F,G, Fig. S3B,C). Taken together, HeyL and Hes1 can form a heterodimer, perhaps to exert their effective functions.

HeyL-Hes1 heterodimer complex binds to more diverse DNA sites than HeyL alone

In order to elucidate the functional difference between HeyL alone and the HeyL-Hes1 heterodimer, chromatin immunoprecipitation (ChIP) assays were performed using doxycycline-dependent HeyL alone or C2C12 cells expressing HeyL-Hes1 (Fig. 5A). HeyL- or Hes1-expressing cells were sorted by EGFP (enhanced green fluorescent protein) or mKO2 (monomeric Kusabira Orange2) fluorescence, respectively (Fig. 5B). A FLAG-tag was fused to *Heyl*, but not *Hes1*; therefore, we used an anti-FLAG antibody for immunoprecipitation assays, followed by sequencing (ChIP-seq). Genome-wide binding profiles showed that there was a notable difference between HeyL alone and HeyL-Hes1 cistromes (Fig. 5C). The number of ChIP-seq peaks for HeyL-Hes1 was constantly greater than that for HeyL alone at various *P*-value thresholds (Fig. 5D), suggesting that HeyL-Hes1 has more binding sites than HeyL alone. Fig. 5E shows the signals for a HeyL-Hes1 heterodimer and HeyL alone along with the histone modifications H3K27ac, H3K27me3 and H3K4me3. HeyL-Hes1 binding sites

Development (2019) 146, dev163618. doi:10.1242/dev.163618

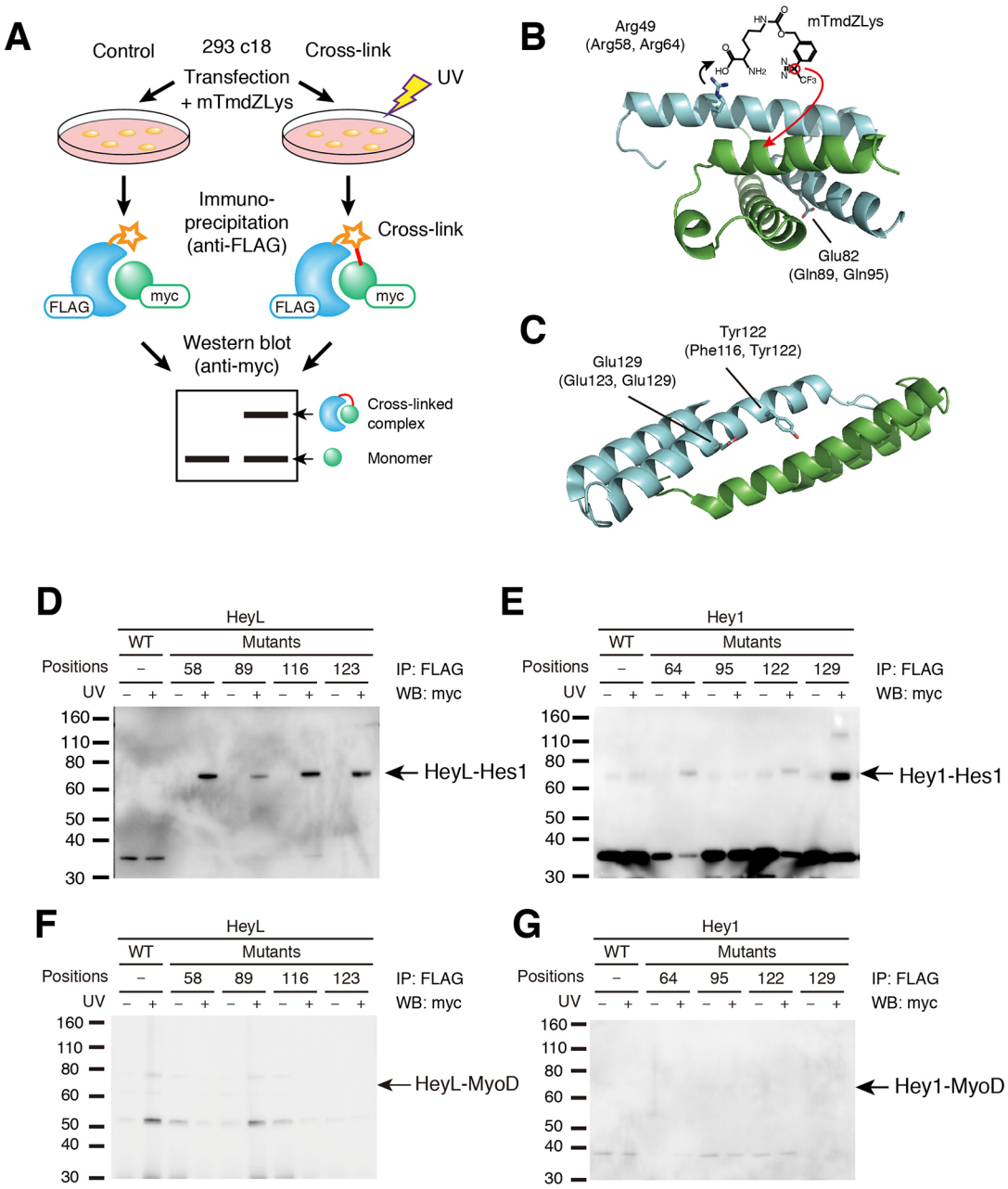

Fig. 4. HeyL forms a heterodimer complex with Hes1 in living cells. (A) Experimental procedure for the photo-crosslinking of heterodimers between Hey1, HeyL, Hes1 and MyoD, and the subsequent analysis. When FLAG-tagged Hey forms a heterodimer with Myc-tagged Hes1 or MyoD, crosslinked complex is detected in response to UV treatment (right flow chart). (B,C) Homodimer complex structures of the human HES1 Orange domain (B) and the human HEY1 bHLH domain (C) obtained from the Protein Data Bank (ID: 2MH3 and 2DB7, respectively). The residue positions chosen for the substitution with mTmdZLys are indicated. The homological residues of mouse HeyL (Orange domain; positions 58 and 89, bHLH domain; positions 116 and 123) and Hey1 (Orange domain; positions 64 and 95, bHLH domain; positions 122 and 129) are indicated in parentheses. (D) Western blotting for analysis of the photo-crosslinking between HeyL-Hes1. Wild-type HeyL (WT) and its mutants containing mTmdZLys at the indicated positions, tagged with FLAG peptide, were co-expressed with Myc-tagged Hes1 in 293 c18 cells. HeyL complexes were immunoprecipitated with an anti-FLAG antibody from extracts of the cells that were exposed or not to UV. Crosslinked complexes of HeyL and Hes1 were detected with an anti-Myc antibody. (E) Western blotting for the analysis of photo-crosslinking of Hey1-FLAG with Hes1-myc (E), HeyL-FLAG with MyoD-myc (F), or Hey1-FLAG with MyoD-myc (G).

overlapped with H3K27ac and H3K4me3, which indicates that HeyL-Hes1 preferentially binds to active proximal promoter regions. Importantly, the list of enriched motifs around HeyL-Hes1 peaks included the cis-element of Hey1, CACGTG, and a Hes1-binding site, CACGCG (Fig. 5F). In the case of HeyL alone, we did not detect enriched motifs with a significant difference. Compared with HeyL alone, the higher signal levels of HeyL-Hes1 in *Hey1* and *Hes1* promoter regions are consistent with the fact that Hey1 and Hes1 negatively regulate their own mRNA expression (Fig. 5G). Chip-PCR analyses of the *Hes1* promoter containing the Hey1-binding site (CACGTG) indicated that HeyL-Hes1 binds to the cis-element of Hey1 more efficiently than HeyL alone, as observed in Hey1 alone or Hey1-Hes1. (Fig. 5H). Chip-PCR analyses of the *Hey1* promoter containing the Hes1-binding site (CACGCG; Hey1 also binds to this motif; Heisig et al., 2012) also showed similar results (Fig. 5H). These results suggest that HeyL

Development (2019) 146, dev163618. doi:10.1242/dev.163618

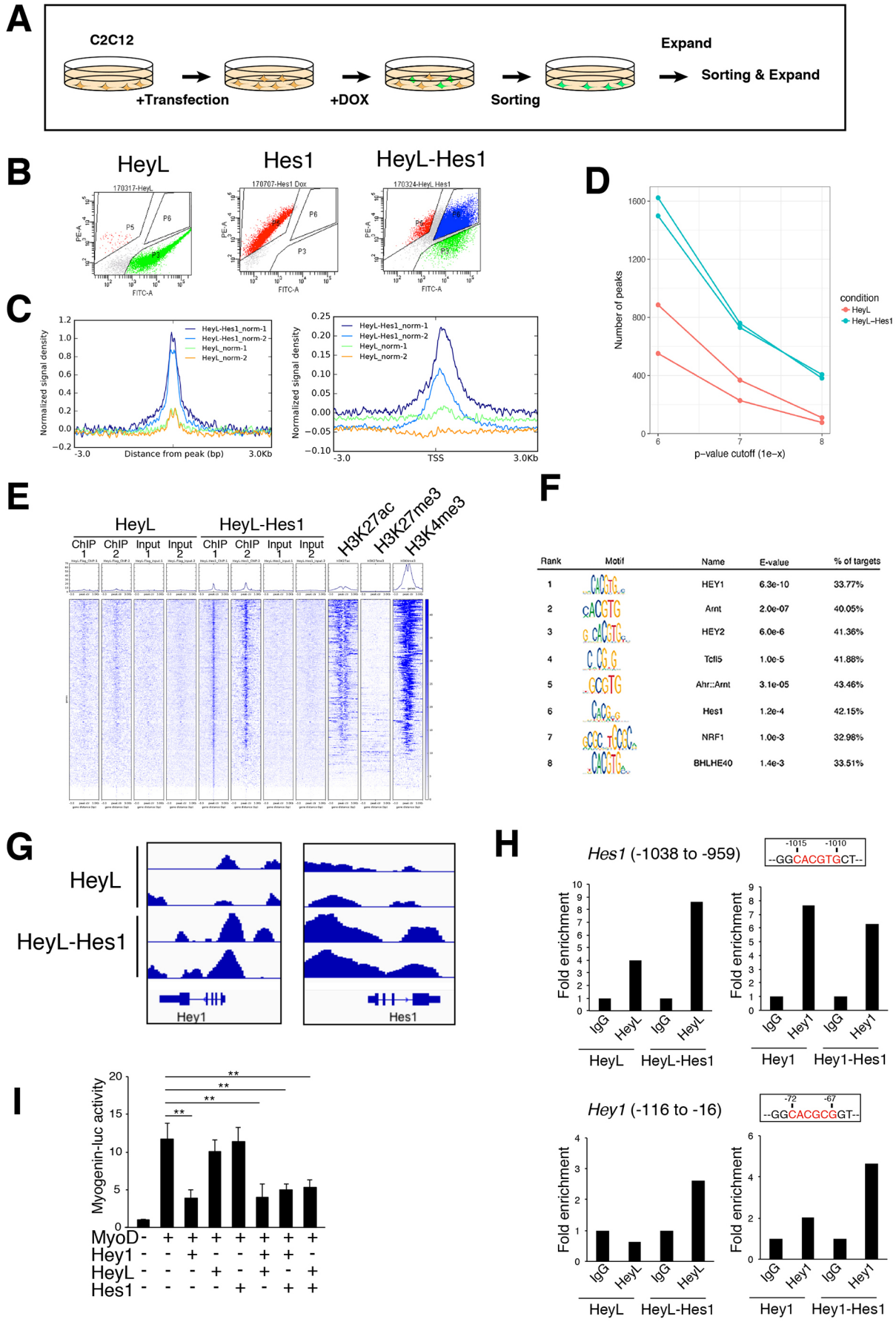

Fig. 5. See next page for legend.

Development (2019) 146, dev163618. doi:10.1242/dev.163618

Fig. 5. Co-existing HeyL and Hes1 bind to diverse DNA sites and exert a synergistic effect. (A) Experimental procedure for the preparation of doxycycline (Dox)-dependent Hey1-, HeyL- or HeyL-Hes1-expressing C2C12 cells. (B) FACS profile of Dox-treated HeyL (EGFP) or HeyL-Hes1 (EGFP and mKO2)-expressing C2C12. The results of Hes1 alone are also shown as the reference for mKO2 fluorescence. (C) Signal distributions of HeyL and Hes1 normalized to the corresponding input data around the peak centers for the union of peaks for four samples (left) and around the transcription start site (TSS) (right). (D) The numbers of HeyL alone and HeyL-Hes1 peaks detected at various *P*-value cutoffs. The number is greater for HeyL-Hes1 for each case. (E) Heat maps for the HeyL alone, HeyL-Hes1, H3K27ac, H3K27me3 and H3K4me3 signals within 3 kb around HeyL-Hes1 peak centers (replicate 1). (F) Enriched motifs identified in regions bound preferentially by HeyL-Hes1. (G) Integrative Genomics Viewer (IGV) images illustrating the signal for HeyL alone and HeyL-Hes1 normalized to the corresponding input signal at *Hey1* and *Hes1* gene loci. Only positive log2 ratios are shown. (H) Chip-PCR analyses were performed using HeyL-, HeyL-Hes1-, Hey1- or Hey1-Hes1-expressing C2C12 cells and control IgG and anti-FLAG antibodies. Immunoprecipitated DNA fragments were analyzed by real-time PCR with specific primers to *Hes1* promoter regions (−1038 to −959 site) containing the 'CACGTG' motif or *Hey1* promoter regions (−116 to −16 site) containing the 'CACGCG' motif. The numbers mean positions relative to the transcriptional initiation site (+1).The average from two to three independent experiments is plotted. (I) Relative luciferase activities of MyoD or MyoD co-transfected with Hey1, HeyL, and/or Hes1 expression plasmids in C2C12. The average of three to five independent experiments with s.d. is plotted. ***P*<0.01.

can bind the Hey1-binding sites in concert with Hes1, which also supports the redundant roles of Hey1 and HeyL in MuSCs.

Finally, we examined the synergistic effects of Hes1 and HeyL using myogenin-promoter activity instead of MyoD for the following reasons: (1) *Myod* mRNA levels were not different between control and dKO/co-dKO; (2) the myogenin promoter includes a Hey1-binding site (Buas et al., 2010); (3) suppression mechanisms of myogenin might be more crucial for MuSCs than those of MyoD because myogenin expression induces irreversible terminal differentiation; (4) recent studies showed that *Myod* mRNA is abundant in quiescent MuSCs (de Morrée et al., 2017). As in the previous report, Hey1 suppressed myogenin promoter activity in a dose-dependent manner. In contrast, neither HeyL nor Hes1 had an effect (Fig. S4). However, the co-existence of HeyL and Hes1 remarkably suppressed myogenin-luciferase activity, indicating that HeyL requires Hes1 to exert the anti-myogenic effect (Fig. 5I).

DISCUSSION

Canonical Notch signaling is an essential pathway for maintaining the undifferentiated state of MuSCs (Bjornson et al., 2012; Fujimaki et al., 2018; Mizuno et al., 2015; Mourikis et al., 2012). However, the downstream effectors exerting the anti-myogenic effects have not been identified. Neither HeyL nor Hes1 has inhibitory effects on myogenic differentiation and myogenic gene expression in a C2C12 cell line (Buas et al., 2009; Shawber et al., 1996), whereas Hey1 has (Buas et al., 2009) (data shown here). Sasai et al. showed that Hes1 inhibited MyoD-induced myogenic conversion of fibroblasts (Sasai et al., 1992). The reported data suggested that Hes1 deprived E47 from MyoD/E47 heterodimer complexes, which inhibited MyoD-induced myogenic conversion. In our and Shawbers' analyses, Hes1 did not inhibit MyoD-dependent myogenin-promoter activity. The discrepancy between Sasai's results and ours could be explained by the dependency of E47 in each analysis. In fact, Sasai et al. showed that Hes1 did not inhibit the function of MyoD homodimers and did not bind to the E-box strongly. Importantly, our results demonstrated that, in contrast to Hes1 alone, the Hes1-HeyL heterodimer binds the E-box strongly.

Notch signaling still exerted an anti-myogenic effect in C2C12 cells in which Hey1 was suppressed by siRNA (Buas et al., 2009), indicating that inhibition of myogenesis by Notch consists of redundant or multiple pathways. Our current study implies that HeyL-Hes1 heterodimers and Hey1 homodimers/heterodimers are two essential units downstream of the canonical Notch pathway in MuSCs (Fig. 6). This model does not explain the full picture of anti-myogenic mechanisms in the Notch pathway. When Hey1, HeyL and Hes1 were silenced in C2C12 cells, the Notch ligand still inhibited *Myod* and myogenin mRNA expression (data not shown), suggesting there are other effectors for the anti-myogenic roles of Notch besides Hey1, HeyL and Hes1. This speculation is supported by observations in *Pax3-Cre::Rbp-J* and our *Hey1/HeyL* dKO mice. The depletion of *Rbp-J* by *Pax3-Cre* produced a severe muscle developmental defect compared with *Hey1/HeyL* dKO mice (Fukada et al., 2011; Vasyutina et al., 2007), indicating that the anti-myogenic effects of canonical Notch signaling during embryogenesis depend on something other than Hey1 and HeyL. Thus, additional members of the Hes/Hey family might also participate in the suppression of embryonic myogenesis, or other mechanisms that do not rely on Hes/Hey factors might be active. However, MuSCs require Hey1 and HeyL for entry into quiescence and for their maintenance.

The formation of heterodimeric complexes by other members of the Hes and Hey family has been described before (Fischer and Gessler, 2007; Iso et al., 2001; Jalali et al., 2011). However, to our knowledge, there is no evidence showing a physiological role of Hes-Hey heterodimer complexes. Our present study is the first that indicates the physiological importance of the HeyL-Hes1 heterodimer for maintaining MuSCs in the undifferentiated state. A remaining question is why HeyL prefers to form a heterodimer with Hes1 rather than forming HeyL homodimers or Hey1-HeyL heterodimers. In addition, we did not succeed in suppressing myogenic differentiation by co-expression of HeyL-Hes1 in C2C12 cells, similar to the results when HeyL or Hes1 were expressed separately (data not shown). Myogenin-luciferase analyses do not depend on the existence of a co-repressor when HeyL-Hes1 occupies MyoD-binding sites. HeyL to DNA binding in ChIP-seq analyses is also independent of the existence of a co-repressor. Collectively, non-myogenic effects of HeyL and Hes1 will result from the absence

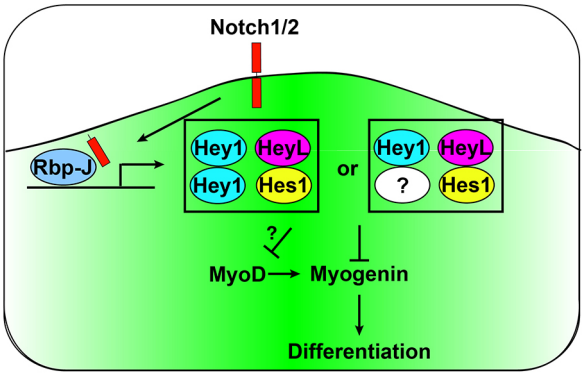

Fig. 6. Hey1, HeyL and Hes1 are required in muscle stem cells for maintaining the undifferentiated state. HeyL-Hes1 heterodimers and Hey1 homodimers/heterodimers are two essential units downstream of the canonical Notch pathway in MuSCs. Hes1 is a potential partner of Hey1, but there is a possibility that Hey1 functions as a homodimer or heterodimer with an unidentified factor. HeyL alone does not bind to Hey1-binding sites, but HeyL-Hes1 binds to these sites. Myogenin could be a direct target of Hey/Hes1 heterodimers/homodimers. *MyoD* is also a potential target of Hey/Hes heterodimers/homodimers, but MyoD mRNA levels are not increased in Hey1/L-mutant MuSCs.

Development (2019) 146, dev163618. doi:10.1242/dev.163618

of a functional co-repressor for Hey1 and Hes1 in C2C12. On the contrary, the existence of a functional co-repressor for Hes1 in the primary myoblast explains the significant anti-myogenic effect of Hes1. The identification of the co-repressor(s) that interact with Hes/Hey factors will lead to a better understanding of the mechanisms that maintain the undifferentiated state of MuSCs.

In this study, we analyzed the myogenin promoter as a target gene of Hes/Hey. In considering an undifferentiated state of MuSCs, the regulatory mechanism of MyoD (upstream of myogenin) expression attracts attention. In *Rbp-J* coKO, *Hey1/HeyL*-double null and *Hey1/HeyL* co-dKO mice, the frequency of $MyoD^{+}$ MuSC was dramatically increased, but mRNA expression of *Myod* was unchanged or decreased in those three KO MuSCs (Bjornson et al., 2012; Fukada et al., 2011; Mourikis et al., 2012). This might indicate that the translation of *Myod* mRNA is accelerated in MuSCs as a result of the loss of canonical Notch signaling. Zismanov et al. reported that phosphorylation of serine 51 of eIF2α is necessary to maintain MuSCs in an undifferentiated and quiescent state (Zismanov et al., 2016). MuSCs unable to phosphorylate eIF2α exited quiescence and activated the myogenic program, which included an upregulation of the MyoD protein level. eIF2α is a key regulator of mRNA translation, which means that *Myod* mRNA is present even in quiescent MuSCs but the protein is not produced, similar to *Myf5*, another myogenic determination gene (Crist et al., 2012). Intriguingly, de Morrée et al. reported that quiescent MuSCs include abundant *Myod* mRNA and an RNA-binding protein, Staufen1 (Stau1), which suppresses the translation of *Myod* mRNA (de Morrée et al., 2017). On the other hand, Machado et al. showed that the *Myod* transcription level in quiescent MuSCs is much weaker than that in activated MuSCs, and the *Myod* transcription level is upregulated during MuSC isolation (Machado et al., 2017). The necessity of transcriptional regulation of MyoD in quiescent MuSCs is controversial, but Hey1, HeyL and Hes1 are candidate factors for suppressing *Myod* transcription because they can suppress the *Myod* transcriptional level in primary myoblasts. Sun et al. reported that Hey1 suppressed MyoD-dependent activation of the myogenin promoter by forming MyoD-Hey1 complexes (Sun et al., 2001). On the other hand, Buas et al. argued against formation of a MyoD-Hey1 complex (Buas et al., 2010). Using photo-crosslinking analyses, we detected neither MyoD-Hey1 nor MyoD-HeyL complexes. Notably, MuSCs do not express MyoD at the protein level; therefore, these results suggest that the anti-myogenic effect of both Hey1 and HeyL in MuSCs are independent of the formation of a heterodimer with MyoD.

We expected that genetic inactivation of *Hey1* would be induced in $Pax7^{CreERT2/+}::Hey1^{flox/-}$ or $^{flox/flox}$ mice by Tm injection. $Pax7^{CreERT2/+}$ mice have been widely used, and we have also reported Tm-dependent depletion of *Calcr* (Yamaguchi et al., 2015). One reason for the unexpected result is the effect of *Pax7* haploinsufficiency because *Pax7* is transcribed from one allele in the $Pax7^{CreERT2/+}$ mice. However, we also had similar results using tomato-RFP mice and $Pax7^{CreERT2/+}$ mice (Fig. S5), suggesting leaky activation of Cre recombinase. The mechanism evoking leaky activation of Cre recombinase is unknown because CreERT2 is a modified enzyme with higher specificity compared with CreER (Indra et al., 1999). However, we observed significant differences in MuSC number between $Pax7^{CreERT2/+}::Hey1^{flox/+}::HeyL^{-/-}$ and $Pax7^{CreERT2/+}::Hey1^{flox/-}$ or $^{flox/flox}::HeyL^{-/-}$ mice with/without Tm, indicating that Hey1 and HeyL are necessary for maintaining MuSCs as well as generating MuSCs during postnatal development.

In conclusion, our results indicate that Hey1 and HeyL maintain the undifferentiated state of MuSCs in a cell-autonomous and redundant manner as effectors of canonical Notch signaling. We also demonstrated here that HeyL requires Hes1 for efficient DNA binding, including at Hey1-binding sites. The undifferentiated state of MuSCs could be defined by non-expression of MyoD, but the transcriptional expression of MyoD in quiescent MuSCs is controversial. Further analyses of MyoD transcriptional regulation and the target genes and co-repressor of HeyL-Hes1 will lead to elucidation of the maintenance mechanisms of MuSCs.

MATERIALS AND METHODS

Mice

$Hey1^{-/-}$ allele and $Heyl^{-/-}$ mice were generated as described previously (Fukada et al., 2011; Kokubo et al., 2005). *Hey1*-floxed mice were generated by Fischer et al. (Fischer et al., 2005). $Pax7^{CreERT2/+}$ (Lepper et al., 2009) mice were obtained from Jackson Laboratories. All procedures for experimental animals were approved by the Experimental Animal Care and Use Committee at Osaka University.

Muscle injury

Muscles were injured by injecting cardiotoxin (2.5 µl per g of mouse body weight of 10 µM in saline; Sigma-Aldrich) into the tibialis anterior (TA) muscle.

Preparation and florescence-activated cell sorting (FACS) analyses of skeletal muscle-derived mononuclear cells

Mononuclear cells from uninjured limb muscles were prepared using 0.2% collagenase type II (Worthington Biochemical Corporation) as previously described (Uezumi et al., 2006).

Mononuclear cells derived from skeletal muscle were stained with FITC-conjugated anti-CD31 (BD Pharmingen, 558738, 1:400), CD45 (Ptprc; eBioscience, 11-0451-82, 1:800), phycoerythrin-conjugated anti-Sca-1 (Ly6a) (BD Pharmingen, 553336, 1:400), and biotinylated-SM/C-2.6 (Fukada et al., 2004) antibodies. Cells were then incubated with streptavidin-labeled allophycocyanin (BD Biosciences) on ice for 30 min, and re-suspended in PBS containing 2% fetal calf serum and 2 µg/ml propidium iodide. Cell sorting was performed using a FACS Aria II flow cytometer (BD Immunocytometry Systems). Debris and dead cells were excluded by forward scatter, side scatter, and propidium iodide gating. Data were collected using FACSDiva software (BD Biosciences).

Single myofiber culture and staining

Single myofibers were isolated from extensor digitorum longus muscles following a previously described protocol (Rosenblatt et al., 1995). Fixation and immunostaining followed described protocols (Shinin et al., 2009). Anti-Pax7 (PAX7-f, 1:2), -MyoD (sc-760, 1:200) and -myogenin (M3559, 1:30) antibodies were purchased from Developmental Studies Hybridoma Bank, Santa Cruz Biotechnology, and Dako (Clone: F5D), respectively. Images were obtained using a BZ-X700 fluorescence microscope (Keyence Osaka, Japan).

RT-PCR

Total RNA was extracted from sorted or cultured cells with a Qiagen RNeasy Mini Kit according to the manufacturer's instructions (Qiagen) and then reverse-transcribed into cDNA using TaqMan Reverse Transcription Reagents (Roche Diagnostics). PCR was performed with cDNA and specific primers. Primer pairs were published in previous reports (Yamaguchi et al., 2015).

Histology

TA muscles were isolated and frozen in liquid nitrogen-cooled isopentane (Wako Pure Chemical Industries). Transverse cryosections (10 µm) were cut with a Leica CM1850 and stained with Hematoxylin and Eosin.

Immunohistochemistry

For immunohistological analyses, transverse cryosections (7 µm) were fixed with 4% paraformaldehyde for 10 min. Anti-Pax7, -MyoD, and -myogenin antibodies were the same as those used in the single myofiber staining. Anti-

Development (2019) 146, dev163618. doi:10.1242/dev.163618

collagen type I and anti-laminin α2 antibody were purchased from Bio-Rad and Enzo Life Sciences (clone 4H8-2), respectively. The anti-M-cadherin antibody was described in a previous study (Yamaguchi et al., 2015). For mouse anti-Pax7, a MOM kit (Vector Laboratories) was used to block endogenous mouse IgG before reaction with the primary antibodies. The signals were recorded photographically using a BZ-X700 fluorescence microscope, and collagen type I-positive areas were quantified using Hybrid Cell Count software (Keyence).

Retroviral vector preparation and infection experiments

The viral particles (retro pCLIG-*Hey1*, pCLIG-*HeyL*, parental retro pCLIG, pMX-*Hes1*, parental retro pMX) were prepared as described (Morita et al., 2000). MuSCs were isolated from C57BL/6 mice, and were plated on dishes coated with Matrigel in growth media (GM). After 3 days, GFP-positive cells were collected by cell sorting. After an additional 2 days culture in GM, the cells were fixed and stained with anti-MyoD antibody (Clone 5.8A, BD Biosciences; 1:200). To examine the effects of Hey1 and HeyL on differentiation of MuSCs, GFP-positive cells were cultured in DM for an additional 3 days, and then stained with anti-sarcomeric α-actinin antibody (Clone: EA-53, Sigma-Aldrich; 1:100).

Photo-crosslinking in living cells

Site-specific incorporation of mTmdZLys into HeyL protein in living cells with an expanded genetic code was performed as described previously (Kita et al., 2016). In brief, a pOriP plasmid containing the *Heyl* gene with an amber nonsense (TAG) mutation in the positions shown in Fig. 4D was transfected into 293 c18 cells, together with the plasmids containing the gene variants for an amber suppressor pyrrolysine tRNA and a mTmdZLys-specific pyrrolysyl-tRNA synthetase. The cells were incubated in DMEM supplemented with mTmdZLys at a final concentration of 10 µM for 16 h, the amino acid was incorporated at the amber position, resulting in the expression of HeyL protein as a full-length form. To analyze heterodimer formation, a pcDNA4/TO plasmid containing the *Hes1* gene was co-transfected with the above-mentioned plasmids. For protein photo-crosslinking, the cells were exposed to UV light (λ=365 nm) for 15 min. Extraction, purification, and western blot analysis of crosslinked products were performed as described previously (Kita et al., 2016). The analyses of the heterodimerization of proteins other than Hey1-Hes1were performed in a similar way.

Doxycyline-inducible Hey and Hes1 construct and cell line selection

Stably expressed clones were obtained through transfections of pT2A-TRETIBI/EGFP-*Hey1*, EGFP-*HeyL* and mKO2-*Hes1* using Lipofectamine 3000 (Life Technologies). C2C12 cells at 20-30% confluence were transfected with an expression vector (4 µg plasmid DNA per 100-mm plate), pCAGGS-TP coding transposase (provided by Dr Kawakami, National Institute of Genetics, Japan) and pT2A-CAG-rtTA2S-M2 and incubated for 24 h. EGFP- or mKO2-positive cells were sorted by a FACS AriaII to select stably expressed clones.

ChIP-seq assay (NGS) and data analysis

ChIP libraries of HeyL alone and HeyL-Hes1 were prepared with the NEBNext Ultra DNA Library Prep Kit for Illumina (New England Biolabs). They were sequenced on an Illumina HiSeq 1500. The reads were then aligned to the mouse reference genome (GRCm38) with the software HISAT2 version 2.0.4 (Kim et al., 2015). Only uniquely mapped reads were considered for subsequent analysis. The aggregation map was prepared using *plotProfile* of the deepTools suite version 2.5.1 (Ramírez et al., 2016). Peaks were identified using the caller BCP version 1.1 (Xing et al., 2012) at various *P*-value cut-offs (*P*-values $<10^{-6}$, 10^{-7} and 10^{-8}, the last of which is the default value). The heat map was drawn with deepTools' *plotHeatmap*, H3K4me3 and H3K27me3 data were obtained from ENCODE (ENCSR000AHO and ENCSR000AHR, respectively) and H3K27ac data from the Rudnicki laboratory (GSE37525) (Blum et al., 2012). Motif enrichment analysis was performed using CentriMo (Bailey and Machanick, 2012); the search was filtered so that it yielded results from the database JASPAR CORE 2016 vertebrates. The target coverage was calculated using the number of region matches.

ChIP-PCR analysis

C2C12 cells were crosslinked with 1% formaldehyde, and sonicated for 15 cycles at 15 s/cycle using a Sonifer Model 250 with an output control of 2 and a duty cycle of 30%. The extract was incubated at 4°C for 24 h with Dynabeads (Invitrogen, 10,003D) pre-coated with 3 µg antibodies against FLAG (Sigma-Aldrich, F1804) and control IgG (Cell Signaling Technology, 5415). The DNA–protein complexes were collected using a magnet, and de-crosslinked in a solution containing 50 mM Tris-HCl (pH 8.0), 10 mM EDTA and 1% sodium dodecyl sulfate. The resulting DNA was analyzed by real-time PCR with specific primers. The specific forward and reverse primers for ChIP-PCR were: 5'-GGG AAG GCG GAG AGG TTG and 5'-CAT GCG GCT GCC AAT CTG for *Hey1* (product size, 100 bp); 5'-GCG GCG GCA ATA AAA CAT CC and 5'-AGC TGC AGT TTG ACA TCA GC for *Hes1* (product size, 79 bp).

Luciferase assay

All vectors were transfected in C2C12 by X-tremeGENE 9 DNA Transfection Reagent (Roche). A 3.8 kb fragment of the myogenin regulatory element was amplified by PCR (Fujisawa-Sehara et al., 1993). The fragment was ligated into a pGL4.23 vector cut with *Xho*I and *Bgl*II, and the sequence was examined. A pRL *Renilla* luciferase reporter vector was used for normalizing the transfection efficiency. Forty hours after transfection, the cells were harvested and lysed using Dual-Luciferase Reporter Assay System (Promega), and then luciferase activity was measured on a GLOMAX-MULTI detection system (Promega). Data indicate the expression relative to the basal level of myogenin-luciferase co-transfected with empty expression vectors.

Statistics

Values were expressed as mean±s.d. Statistical significance was assessed by Student's *t*-test. In comparisons of more than two groups, non-repeated measures analysis of variance (ANOVA) followed by the Bonferroni test (versus control) or SNK test (multiple comparisons) were used. A probability of less than 5% ($P<0.05$) or 1% ($P<0.01$) was considered statistically significant.

Acknowledgement

We sincerely thank Prof. Toshio Kitamura for providing the pMXs vector and packaging cells. We also thank Prof. Ryoichiro Kageyama for pCLIG-Hey1, -HeyL vectors; Dr Kensaku Sakamoto and Dr Shigeyuki Yokoyama for pOriP vectors; and Prof. Seiji Takashima for providing mTmdZLys. We thank Katherine Ono for comments on the manuscript.

Competing interests

The authors declare no competing or financial interests.

Author contributions

Conceptualization: Y. Ohkawa, S.F.; Methodology: N.H., J.N., S.T., T.S., K.I., A.H., A.U., S.F.; Software: J.N., Y. Ohkawa; Validation: A.H., Y. Ohkawa, S.F.; Formal analysis: Y.N., M.N., S.T., A.H., Y. Ohkawa, S.F.; Investigation: Y.N., M.N., N.H., J.N., S.T., L.Z., T.T., K.I., Y. Okada, T.D., A.H., A.U., S.F.; Resources: J.N., T.S., T.T., K.I., Y. Okada, T.D., H.K., M.G., Y. Ohkawa; Data curation: Y.N., M.N., N.H., J.N., A.H., S.F.; Writing - original draft: N.H., J.N., Y. Ohkawa, S.F.; Writing - review & editing: S.F.; Visualization: S.F.; Supervision: S.F.; Project administration: S.F.; Funding acquisition: K.T., S.F.

Funding

This work was supported by a Grant-in Aid for Young Scientists (A) (S.F.) and a Grant-in-Aid for Scientific Research (B) (S.F.) from the Japan Society for the Promotion of Science; an Intramural Research Grant for Neurological and Psychiatric Disorders from the National Center of Neurology and Psychiatry (S.F.); the Suzuken Memorial Foundation (S.F.); and the Japan Agency for Medical Research and Development (18am0101084j0002 to K.T.).

Data availability

ChIP-seq data have been deposited in DNA Databank of Japan (DDBJ) under accession number DRA006432.

Supplementary information

Supplementary information available online at
http://dev.biologists.org/lookup/doi/10.1242/dev.163618.supplemental

References

Bailey, T. L. and Machanick, P. (2012). Inferring direct DNA binding from ChIP-seq. *Nucleic Acids Res.* **40**, e128.

Bjornson, C. R. R., Cheung, T. H., Liu, L., Tripathi, P. V., Steeper, K. M. and Rando, T. A. (2012). Notch signaling is necessary to maintain quiescence in adult muscle stem cells. *Stem Cells* **30**, 232-242.

Blum, R., Vethantham, V., Bowman, C., Rudnicki, M. and Dynlacht, B. D. (2012). Genome-wide identification of enhancers in skeletal muscle: the role of MyoD1. *Genes Dev.* **26**, 2763-2779.

Buas, M. F., Kabak, S. and Kadesch, T. (2009). Inhibition of myogenesis by Notch: evidence for multiple pathways. *J. Cell. Physiol.* **218**, 84-93.

Buas, M. F., Kabak, S. and Kadesch, T. (2010). The Notch effector Hey1 associates with myogenic target genes to repress myogenesis. *J. Biol. Chem.* **285**, 1249-1258.

Cheung, T. H. and Rando, T. A. (2013). Molecular regulation of stem cell quiescence. *Nat. Rev. Mol. Cell Biol.* **14**, 329-340.

Collins, C. A., Olsen, I., Zammit, P. S., Heslop, L., Petrie, A., Partridge, T. A. and Morgan, J. E. (2005). Stem cell function, self-renewal, and behavioral heterogeneity of cells from the adult muscle satellite cell niche. *Cell* **122**, 289-301.

Crist, C. G., Montarras, D. and Buckingham, M. (2012). Muscle satellite cells are primed for myogenesis but maintain quiescence with sequestration of Myf5 mRNA targeted by microRNA-31 in mRNP granules. *Cell Stem Cell* **11**, 118-126.

de Morrée, A., van Velthoven, C. T. J., Gan, Q., Salvi, J. S., Klein, J. D. D., Akimenko, I., Quarta, M., Biressi, S. and Rando, T. A. (2017). Staufen1 inhibits MyoD translation to actively maintain muscle stem cell quiescence. *Proc. Natl. Acad. Sci. USA* **114**, E8996-E9005.

Fischer, A. and Gessler, M. (2007). Delta-Notch–and then? Protein interactions and proposed modes of repression by Hes and Hey bHLH factors. *Nucleic Acids Res.* **35**, 4583-4596.

Fischer, A., Klattig, J., Kneitz, B., Diez, H., Maier, M., Holtmann, B., Englert, C. and Gessler, M. (2005). Hey basic helix-loop-helix transcription factors are repressors of GATA4 and GATA6 and restrict expression of the GATA target gene ANF in fetal hearts. *Mol. Cell. Biol.* **25**, 8960-8970.

Fischer, A., Steidl, C., Wagner, T. U., Lang, E., Jakob, P. M., Friedl, P., Knobeloch, K.-P. and Gessler, M. (2007). Combined loss of Hey1 and HeyL causes congenital heart defects because of impaired epithelial to mesenchymal transition. *Circ. Res.* **100**, 856-863.

Fujimaki, S., Seko, D., Kitajima, Y., Yoshioka, K., Tsuchiya, Y., Masuda, S. and Ono, Y. (2018). Notch1 and Notch2 coordinately regulate stem cell function in the quiescent and activated states of muscle satellite cells. *Stem Cells* **36**, 278-285.

Fujisawa-Sehara, A., Hanaoka, K., Hayasaka, M., Hiromasa-Yagami, T. and Nabeshima, Y. (1993). Upstream region of the myogenin gene confers transcriptional activation in muscle cell lineages during mouse embryogenesis. *Biochem. Biophys. Res. Commun.* **191**, 351-356.

Fukada, S., Higuchi, S., Segawa, M., Koda, K., Yamamoto, Y., Tsujikawa, K., Kohama, Y., Uezumi, A., Imamura, M., Miyagoe-Suzuki, Y. et al. (2004). Purification and cell-surface marker characterization of quiescent satellite cells from murine skeletal muscle by a novel monoclonal antibody. *Exp. Cell Res.* **296**, 245-255.

Fukada, S., Yamaguchi, M., Kokubo, H., Ogawa, R., Uezumi, A., Yoneda, T., Matev, M. M., Motohashi, N., Ito, T., Zolkiewska, A. et al. (2011). Hesr1 and Hesr3 are essential to generate undifferentiated quiescent satellite cells and to maintain satellite cell numbers. *Development* **138**, 4609-4619.

Fukada, S., Ma, Y., Ohtani, T., Watanabe, Y., Murakami, S. and Yamaguchi, M. (2013). Isolation, characterization, and molecular regulation of muscle stem cells. *Front. Physiol.* **4**, 317.

Heisig, J., Weber, D., Englberger, E., Winkler, A., Kneitz, S., Sung, W.-K., Wolf, E., Eilers, M., Wei, C.-L. and Gessler, M. (2012). Target gene analysis by microarrays and chromatin immunoprecipitation identifies HEY proteins as highly redundant bHLH repressors. *PLoS Genet.* **8**, e1002728.

Hino, N., Okazaki, Y., Kobayashi, T., Hayashi, A., Sakamoto, K. and Yokoyama, S. (2005). Protein photo-cross-linking in mammalian cells by site-specific incorporation of a photoreactive amino acid. *Nat. Methods* **2**, 201-206.

Indra, A. K., Warot, X., Brocard, J., Bornert, J.-M., Xiao, J.-H., Chambon, P. and Metzger, D. (1999). Temporally-controlled site-specific mutagenesis in the basal layer of the epidermis: comparison of the recombinase activity of the tamoxifen-inducible Cre-ER(T) and Cre-ER(T2) recombinases. *Nucleic Acids Res.* **27**, 4324-4327.

Iso, T., Sartorelli, V., Poizat, C., Iezzi, S., Wu, H.-Y., Chung, G., Kedes, L. and Hamamori, Y. (2001). HERP, a novel heterodimer partner of HES/E(spl) in Notch signaling. *Mol. Cell. Biol.* **21**, 6080-6089.

Iso, T., Kedes, L. and Hamamori, Y. (2003). HES and HERP families: multiple effectors of the Notch signaling pathway. *J. Cell. Physiol.* **194**, 237-255.

Jalali, A., Bassuk, A. G., Kan, L., Israsena, N., Mukhopadhyay, A., McGuire, T. and Kessler, J. A. (2011). HeyL promotes neuronal differentiation of neural progenitor cells. *J. Neurosci. Res.* **89**, 299-309.

Kato, H., Taniguchi, Y., Kurooka, H., Minoguchi, S., Sakai, T., Nomura-Okazaki, S., Tamura, K. and Honjo, T. (1997). Involvement of RBP-J in biological functions of mouse Notch1 and its derivatives. *Development* **124**, 4133-4141.

Kim, D., Langmead, B. and Salzberg, S. L. (2015). HISAT: a fast spliced aligner with low memory requirements. *Nat. Methods* **12**, 357-360.

Kita, A., Hino, N., Higashi, S., Hirota, K., Narumi, R., Adachi, J., Takafuji, K., Ishimoto, K., Okada, Y., Sakamoto, K. et al. (2016). Adenovirus vector-based incorporation of a photo-cross-linkable amino acid into proteins in human primary cells and cancerous cell lines. *Sci. Rep.* **6**, 36946.

Kokubo, H., Miyagawa-Tomita, S., Nakazawa, M., Saga, Y. and Johnson, R. L. (2005). Mouse hesr1 and hesr2 genes are redundantly required to mediate Notch signaling in the developing cardiovascular system. *Dev. Biol.* **278**, 301-309.

Kuroda, K., Tani, S., Tamura, K., Minoguchi, S., Kurooka, H. and Honjo, T. (1999). Delta-induced Notch signaling mediated by RBP-J inhibits MyoD expression and myogenesis. *J. Biol. Chem.* **274**, 7238-7244.

Lai, E. C. (2004). Notch signaling: control of cell communication and cell fate. *Development* **131**, 965-973.

Lepper, C., Conway, S. J. and Fan, C.-M. (2009). Adult satellite cells and embryonic muscle progenitors have distinct genetic requirements. *Nature* **460**, 627-631.

Lepper, C., Partridge, T. A. and Fan, C.-M. (2011). An absolute requirement for Pax7-positive satellite cells in acute injury-induced skeletal muscle regeneration. *Development* **138**, 3639-3646.

Lindsell, C. E., Shawber, C. J., Boulter, J. and Weinmaster, G. (1995). Jagged: a mammalian ligand that activates Notch1. *Cell* **80**, 909-917.

Machado, L., Esteves de Lima, J., Fabre, O., Proux, C., Legendre, R., Szegedi, A., Varet, H., Ingerslev, L. R., Barres, R., Relaix, F. et al. (2017). In situ fixation redefines quiescence and early activation of skeletal muscle stem cells. *Cell Rep.* **21**, 1982-1993.

Mizuno, S., Yoda, M., Shimoda, M., Tohmonda, T., Okada, Y., Toyama, Y., Takeda, S., Nakamura, M., Matsumoto, M. and Horiuchi, K. (2015). A disintegrin and metalloprotease 10 (ADAM10) is indispensable for maintenance of the muscle satellite cell pool. *J. Biol. Chem.* **290**, 28456-28464.

Morita, S., Kojima, T. and Kitamura, T. (2000). Plat-E: an efficient and stable system for transient packaging of retroviruses. *Gene Ther.* **7**, 1063-1066.

Mourikis, P., Sambasivan, R., Castel, D., Rocheteau, P., Bizzarro, V. and Tajbakhsh, S. (2012). A critical requirement for Notch signaling in maintenance of the quiescent skeletal muscle stem cell state. *Stem Cells* **30**, 243-252.

Nakagawa, O., McFadden, D. G., Nakagawa, M., Yanagisawa, H., Hu, T., Srivastava, D. and Olson, E. N. (2000). Members of the HRT family of basic helix-loop-helix proteins act as transcriptional repressors downstream of Notch signaling. *Proc. Natl. Acad. Sci. USA* **97**, 13655-13660.

Ramírez, F., Ryan, D. P., Grüning, B., Bhardwaj, V., Kilpert, F., Richter, A. S., Heyne, S., Dündar, F. and Manke, T. (2016). deepTools2: a next generation web server for deep-sequencing data analysis. *Nucleic Acids Res.* **44**, W160-W165.

Rosenblatt, J. D., Lunt, A. I., Parry, D. J. and Partridge, T. A. (1995). Culturing satellite cells from living single muscle fiber explants. *In Vitro Cell. Dev. Biol. Anim.* **31**, 773-779.

Sacco, A., Doyonnas, R., Kraft, P., Vitorovic, S. and Blau, H. M. (2008). Self-renewal and expansion of single transplanted muscle stem cells. *Nature* **456**, 502-506.

Sambasivan, R., Yao, R., Kissenpfennig, A., Van Wittenberghe, L., Paldi, A., Gayraud-Morel, B., Guenou, H., Malissen, B., Tajbakhsh, S. and Galy, A. (2011). Pax7-expressing satellite cells are indispensable for adult skeletal muscle regeneration. *Development* **138**, 3647-3656.

Sasai, Y., Kageyama, R., Tagawa, Y., Shigemoto, R. and Nakanishi, S. (1992). Two mammalian helix-loop-helix factors structurally related to Drosophila hairy and Enhancer of split. *Genes Dev.* **6**, 2620-2634.

Shawber, C., Nofziger, D., Hsieh, J. J., Lindsell, C., Bogler, O., Hayward, D. and Weinmaster, G. (1996). Notch signaling inhibits muscle cell differentiation through a CBF1-independent pathway. *Development* **122**, 3765-3773.

Shinin, V., Gayraud-Morel, B. and Tajbakhsh, S. (2009). Template DNA-strand co-segregation and asymmetric cell division in skeletal muscle stem cells. *Methods Mol. Biol.* **482**, 295-317.

Sun, J., Kamei, C. N., Layne, M. D., Jain, M. K., Liao, J. K., Lee, M.-E. and Chin, M. T. (2001). Regulation of myogenic terminal differentiation by the hairy-related transcription factor CHF2. *J. Biol. Chem.* **276**, 18591-18596.

Uezumi, A., Ojima, K., Fukada, S., Ikemoto, M., Masuda, S., Miyagoe-Suzuki, Y. and Takeda, S. (2006). Functional heterogeneity of side population cells in skeletal muscle. *Biochem. Biophys. Res. Commun.* **341**, 864-873.

Vasyutina, E., Lenhard, D. C., Wende, H., Erdmann, B., Epstein, J. A. and Birchmeier, C. (2007). RBP-J (Rbpsuh) is essential to maintain muscle progenitor cells and to generate satellite cells. *Proc. Natl. Acad. Sci. USA* **104**, 4443-4448.

Wen, Y., Bi, P., Liu, W., Asakura, A., Keller, C. and Kuang, S. (2012). Constitutive Notch activation upregulates Pax7 and promotes the self-renewal of skeletal muscle satellite cells. *Mol. Cell. Biol.* **32**, 2300-2311.

White, R. B., Biérinx, A.-S., Gnocchi, V. F. and Zammit, P. S. (2010). Dynamics of muscle fibre growth during postnatal mouse development. *BMC Dev. Biol.* **10**, 21.

Xing, H., Mo, Y., Liao, W. and Zhang, M. Q. (2012). Genome-wide localization of protein-DNA binding and histone modification by a Bayesian change-point method with ChIP-seq data. *PLoS Comput. Biol.* **8**, e1002613.

Development (2019) 146, dev163618. doi:10.1242/dev.163618

Yamaguchi, M., Watanabe, Y., Ohtani, T., Uezumi, A., Mikami, N., Nakamura, M., Sato, T., Ikawa, M., Hoshino, M., Tsuchida, K. et al. (2015). Calcitonin receptor signaling inhibits muscle stem cells from escaping the quiescent state and the niche. *Cell Reports* **13**, 302-314.

Zismanov, V., Chichkov, V., Colangelo, V., Jamet, S., Wang, S., Syme, A., Koromilas, A. E. and Crist, C. (2016). Phosphorylation of eIF2alpha is a translational control mechanism regulating muscle stem cell quiescence and self-renewal. *Cell Stem Cell* **18**, 79-90.

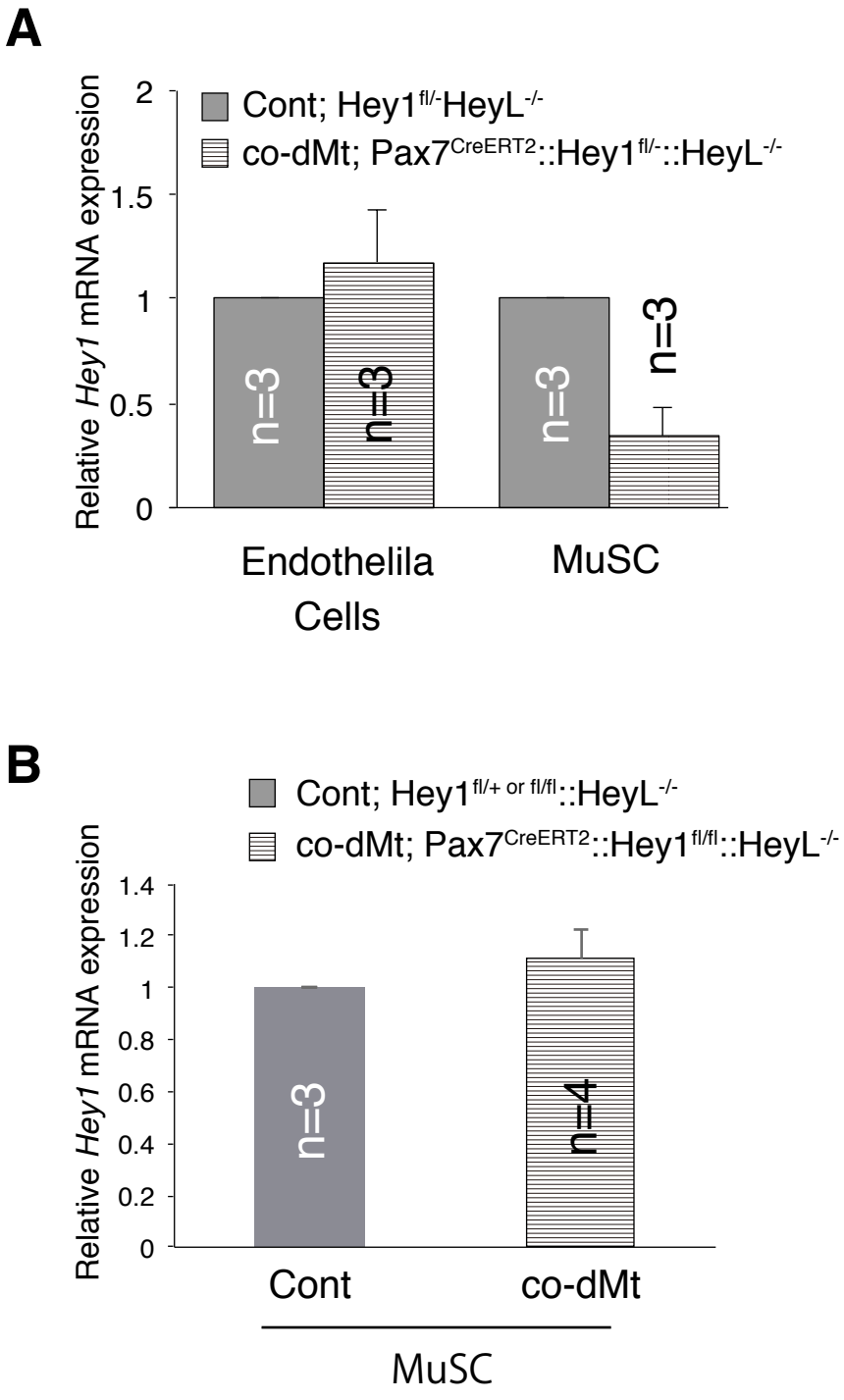

Figure S1. Hey1 mRNA levels of 4- or 9-week-old mice

A; Reduced Hey1 mRNA expression in muscle stem cells, but not in endothelial cells

Relative mRNA expression of *Hey1* gene in freshly isolated MuSCs and endothelial cells derived from Cont (Gray bar; $Hey1^{flox/-}$::$HeyL^{-/-}$) or co-dMt (Stripe bar; $Pax7^{CreERT2/+}$::$Hey1^{flox/- \text{ or } flox/flox}$::$HeyL^{-/-}$ without Tm) mice at 9 weeks old.

B: Hey1 mRNA expression is not changed in co-dMt untreated with tamoxifen at 4 weeks old.

Relative mRNA expression of the *Hey1* gene in freshly isolated MuSCs from Cont (Gray bar; $Hey1^{flox/-}$::$HeyL^{-/-}$) or co-dMt (Stripe bar; $Pax7^{CreERT2/+}$::$Hey1^{flox/- \text{ or } flox/flox}$::$HeyL^{-/-}$ without Tm) mice at 4 weeks old.

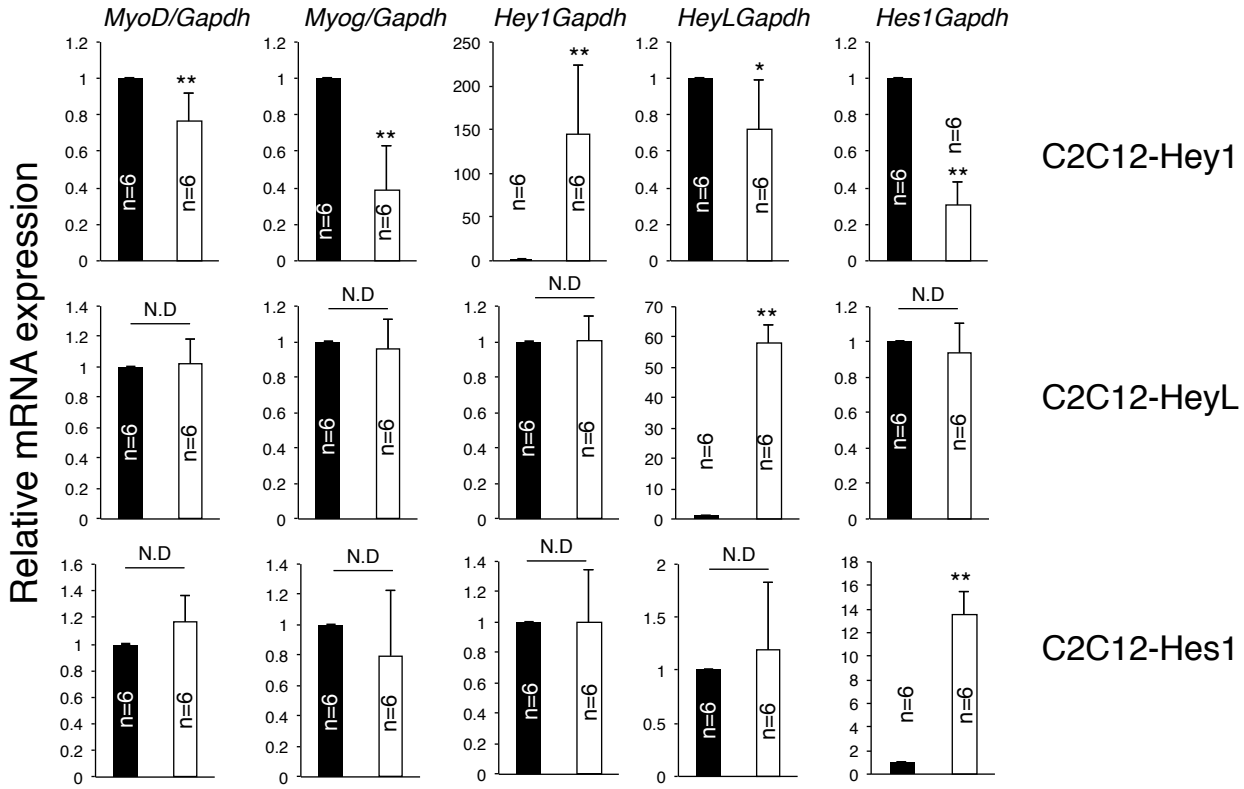

Figure S2. Hey1 has anti-myogenic effect, but not HeyL and Hes1

Relative mRNA expression of indicated genes in control (Black bar; Dox-) or Hey1, HeyL, or Hes1 expressing C2C12 (White bar; Dox+). *; P<0.05; **, P<0.01.

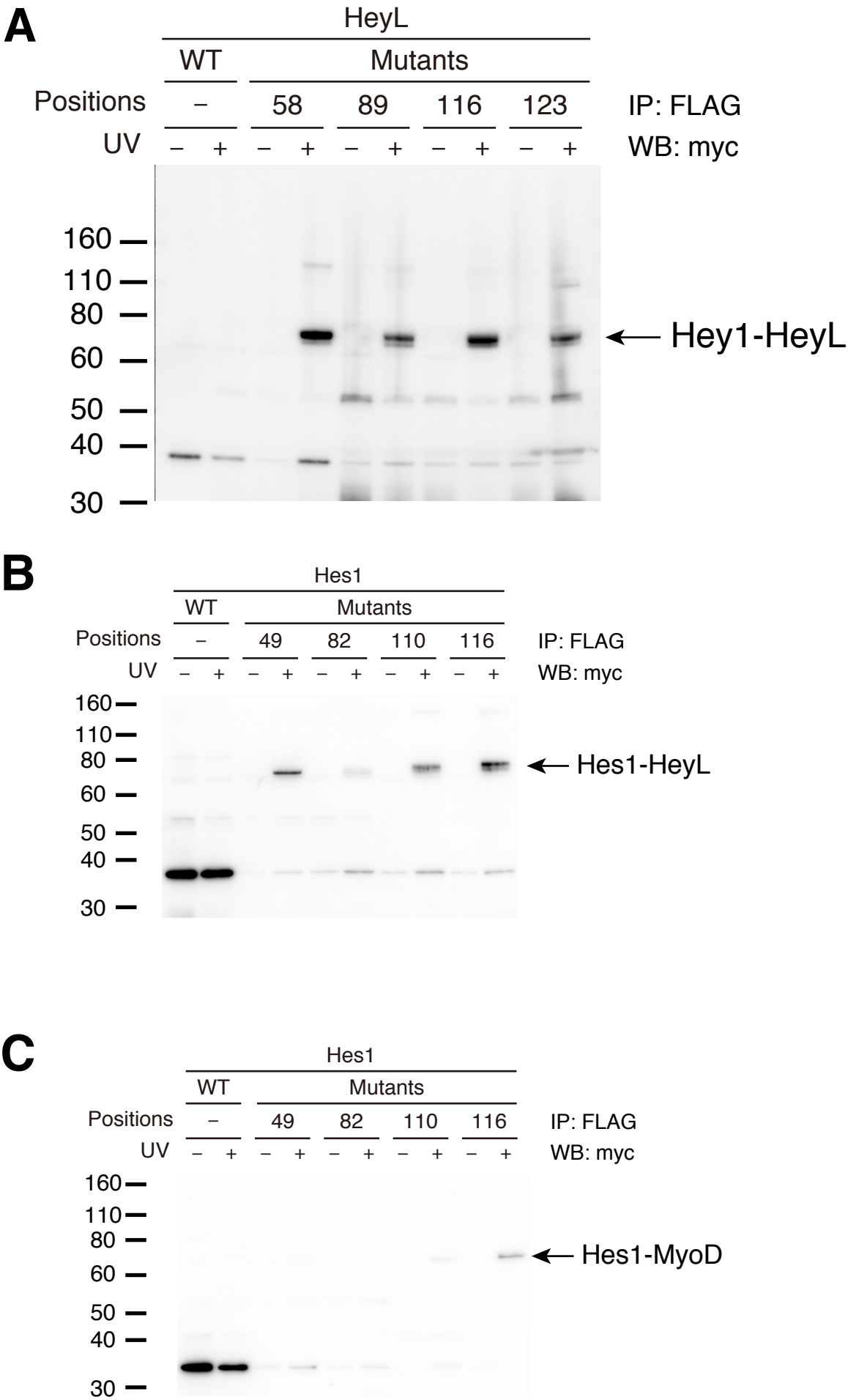

Figure S3. HeyL forms a heterodimer complex with Hey1 in living cells

A: Western blotting for analysis of photo-cross-linking of HeyL-FLAG with Hey1-myc. Site-specific incorporation of mTmdZLys into the Orange (positions 58 and 89) and bHLH (positions 116 and 123) domains of HeyL in 293 c18 cells, protein photo-cross-linking in the cells, and subsequent purification and detection of cross-linked products were performed as described in Figure 4.

B, C: Western blotting for analysis of photo-cross-linking of Hes1-FLAG with HeyL-myc (B), and of Hes1-FLAG with MyoD-myc (C). Site-specific incorporation of mTmdZLys into the Orange (positions 49 and 82) and bHLH (positions 110 and 116) domains of Hes1 in 293 c18 cells, protein photo-cross-linking in the cells, and subsequent purification and detection of cross-linked products were performed as described in Figure 4. While cross-linked complexes between Hes1 and HeyL were clearly detected at about 70 kDa (B), complexes between Hes1 and MyoD were only faintly detected (C). These results indicated that Hes1 interacted with MyoD much less efficiently than with HeyL in the 293 c18 cells.

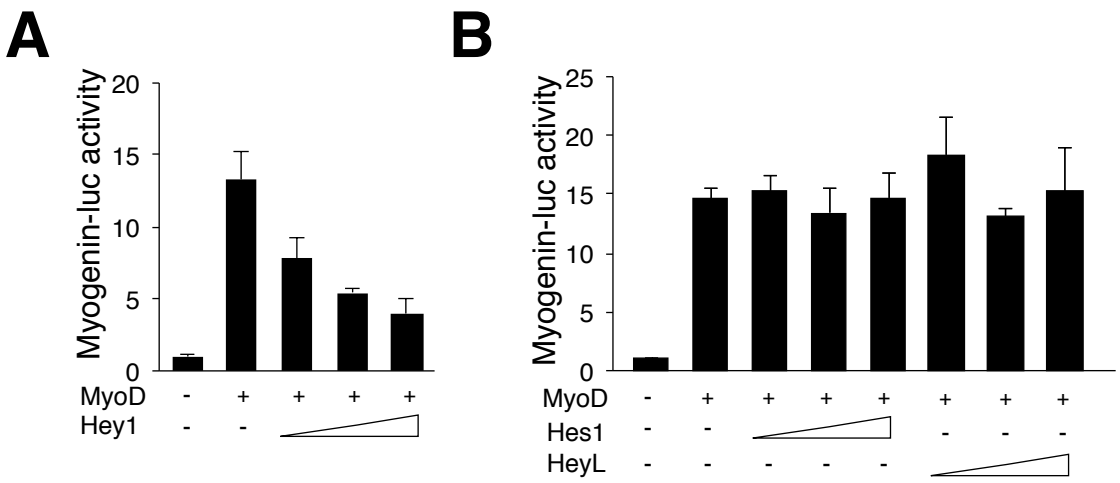

Figure S4. HeyL or Hes1 alone did not suppress MyoD-dependent myogenin promoter activity

A: Relative myogenin-luciferase activities in MyoD cells transfected or co-transfected cells with Hey1 expression plasmids in C2C12. The Y-axis indicates the average results from four independent experiments with SD. **, P<0.01.

B: Relative myogenin-luciferase activities in MyoD cells transfected or co-transfected with HeyL or Hes1 expression plasmids in C2C12. The Y-axis indicates the average results from four independent experiments with SD. **, P<0.01.

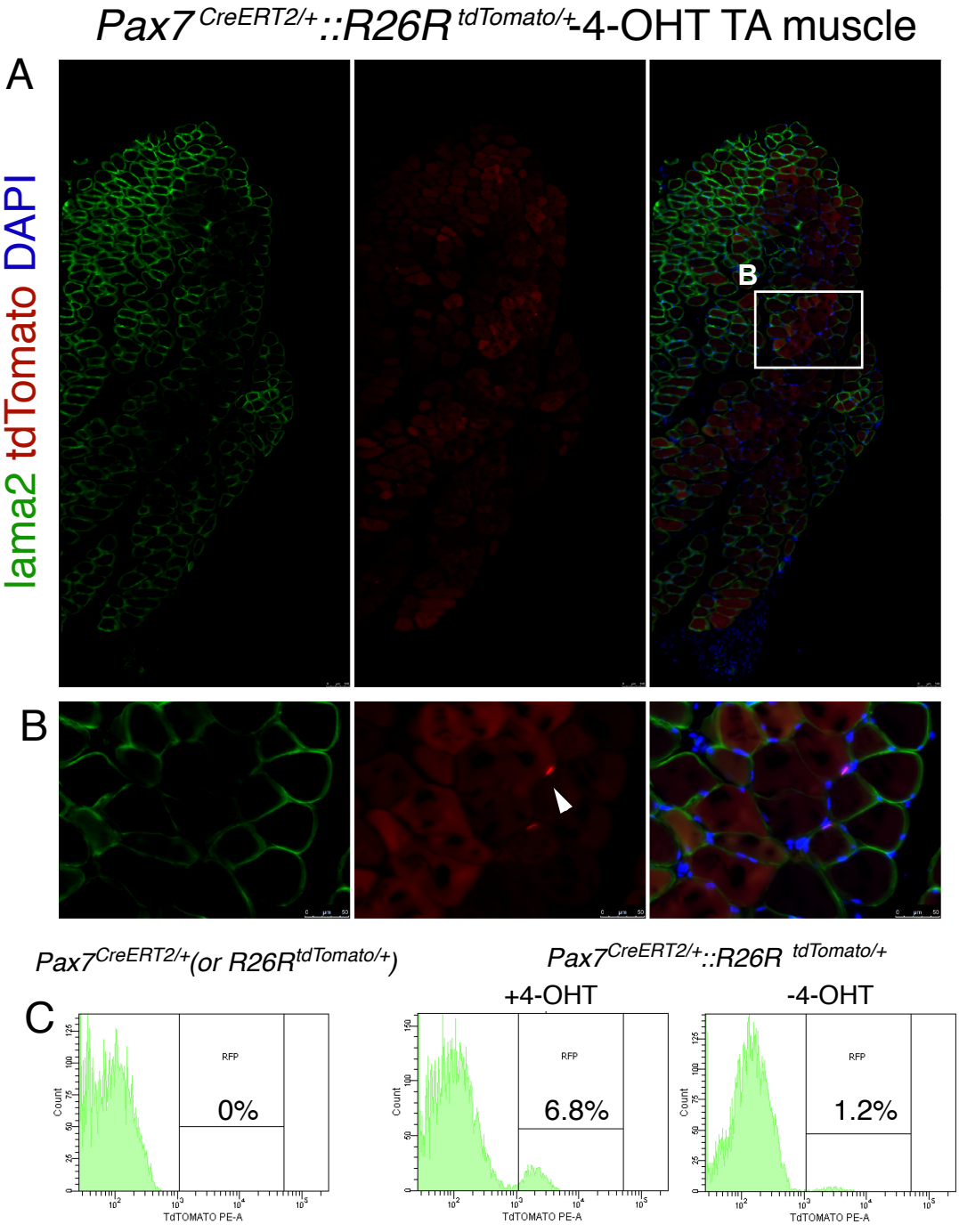

Figure S5. Tamoxifen-independent Cre recombination in *Pax7*$^{CreERT2/+}$ mice::*R26R*$^{tdtomato/+}$.

A, B: Uninjured tibialis anterior muscle (TA) of 4-hydroxy tamoxifen (4-OHT) untreated *Pax7*$^{CreERT2/+}$ mice::*R26R*$^{tdtomato/+}$ mice were stained with anti-laminin α2 (lama2; green) antibody and DAPI (blue). Arrowheads show muscle stem cells expressing tdTomoto (red) (B, magnified image of A) in 4-OHT untreated *Pax7*$^{CreERT2/+}$ mice::*R26R*$^{tdtomato/+}$ mice.

C: The frequency of tdTomato-positive muscle stem cells in control (*Pax7*$^{CreERT2/+}$ or *R26R*$^{tdtomato/+}$ mice), 4-OHT-treated (+4-OHT), or untreated (-4-OHT) *Pax7*$^{CreERT2/+}$ mice::*R26R*$^{tdtomato/+}$ mice.